Journal of Asian Earth Sciences 232 (2022) 104978

Contents lists available at ScienceDirect

Journal of Asian Earth Sciences

journal homepage: www.elsevier.com/locate/jseaes

Provenance of late Paleozoic sedimentary rocks in eastern Kazakhstan: Implications for the collision of the Siberian margin with the Kazakhstan collage

Wanwan Hu [a,b,c], Pengfei Li [a,b,*], Min Sun [d], Inna Safonova [e,f], Yingde Jiang [a,b], Chao Yuan [a,b], Pavel Kotler [e,f]

[a] State Key Laboratory of Isotope Geochemistry, Guangzhou Institute of Geochemistry, Chinese Academy of Sciences, Guangzhou 510640, China
[b] CAS Center for Excellence in Deep Earth Science, Guangzhou 510640, China
[c] University of Chinese Academy of Sciences, Beijing 100049, China
[d] Department of Earth Sciences, The University of Hong Kong, Pokfulam Road, Hong Kong, China
[e] Sobolev Institute of Geology and Mineralogy, SB RAS, Koptyuga Ave. 3, Novosibirsk 630090, Russia
[f] Novosibirsk State University, Pirogova St. 1, Novosibirsk 630090, Russia

ARTICLE INFO

Keywords:
Central Asian Orogenic Belt
Char Shear Zone
Zharma-Saur Arc
Irtysh-Zaisan Complex
Detrital zircon

ABSTRACT

To unravel when, where, and how multiple arc systems were amalgamated is crucial for understanding the accretion processes of the Central Asian Orogenic Belt. Here we focus on the collision of the Siberian margin and the Kazakhstan collage along the Char Shear/Suture Zone in eastern Kazakhstan. We conducted U–Pb dating and Hf isotope analysis for detrital zircons of clastic rocks across the collisional zone of the Siberian margin (the Irtysh-Zaisan Complex) and the Kazakhstan collage (the Zharma-Saur Arc and the Char Zone). Our results show that the Irtysh-Zaisan Complex carries abundant early Paleozoic detrital zircons and minor Precambrian zircons, but there is a lack of such zircon populations in the Zharma-Saur Arc and the Char Zone. Devonian to Carboniferous detrital zircons appear in all sampling tectonic units, in which $\varepsilon_{Hf}(t)$ values of Carboniferous zircons from the Zharma-Saur Arc and the Char Zone are characterized by a narrow range (~10–17) that is different from a relatively wider range of $\varepsilon_{Hf}(t)$ values of ~5–18 for the Carboniferous zircons in the Irtysh-Zaisan Complex. The distinct sedimentary provenances of the Irtysh-Zaisan Complex and the Zharma-Saur Arc/Char Zone confirm that their tectonic boundary lies along the Char Shear Zone in eastern Kazakhstan. As the Late Carboniferous sedimentary rocks from the Zharma-Saur Arc and the Char Zone do not receive detritus from the Siberian margin, we consider that the Ob-Zaisan Ocean between the Siberian margin and the Kazakhstan collage was closed later than the deposition of these sedimentary rocks (<321 Ma).

1. Introduction

The Central Asian Orogenic Belt (CAOB), as a typical accretionary orogen, occupies most of the central Asian interior. The accretion processes and mechanisms of this giant orogenic system has attracted widespread attention in the past decades (Zonenshain et al., 1990; Şengör et al., 1993; Windley et al., 2007; Wilhem et al., 2012; Li et al., 2013; Han et al., 2015; Xiao et al., 2015, 2018; Li et al., 2019). An archipelago paleographic configuration has been proposed for the CAOB during the Paleozoic, in which multiple Andean-, Japanese-, Alaska-, Mariana-type arc systems were developed synchronously (Xiao et al., 2010, 2013; Safonova et al., 2011, 2018; Wilhem et al., 2012). These arc systems were amalgamated following the closure of the Paleo-Asian Ocean (PAO) in the latest Paleozoic, which was accompanied by the occurrence of several large-scale of strike-slip shear zones (Fig. 1a; Qu and Zhang, 1991, 1994; Şengör et al., 1993; Allen et al., 1995; Shu et al., 1999; Travin et al., 2001; Laurent-Charvet et al., 2003; Buslov et al., 2004; Li et al., 2017; Han and Zhao, 2018; Hu et al., 2020). This collisional phase significantly obliterated earlier accretion-related records, and modified the architecture of the CAOB. Therefore, it is crucial firstly to unravel when, where and how multiple arc systems were amalgamated in order to understand the accretion mechanisms of the CAOB.

* Corresponding author at: State Key Laboratory of Isotope Geochemistry, Guangzhou Institute of Geochemistry, Chinese Academy of Sciences, Guangzhou 510640, China.
E-mail address: pengfeili@gig.ac.cn (P. Li).

https://doi.org/10.1016/j.jseaes.2021.104978
Received 30 May 2021; Received in revised form 10 October 2021; Accepted 14 October 2021
Available online 25 October 2021

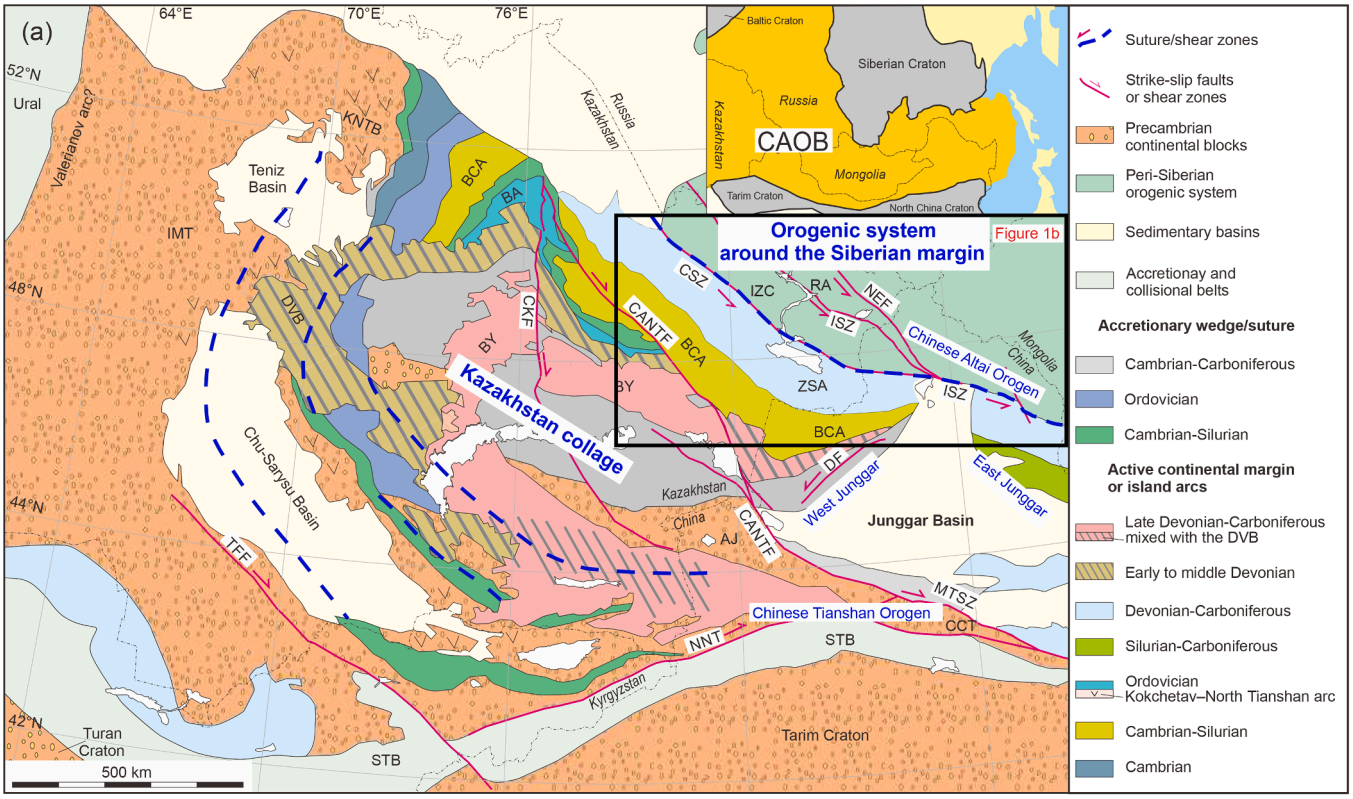

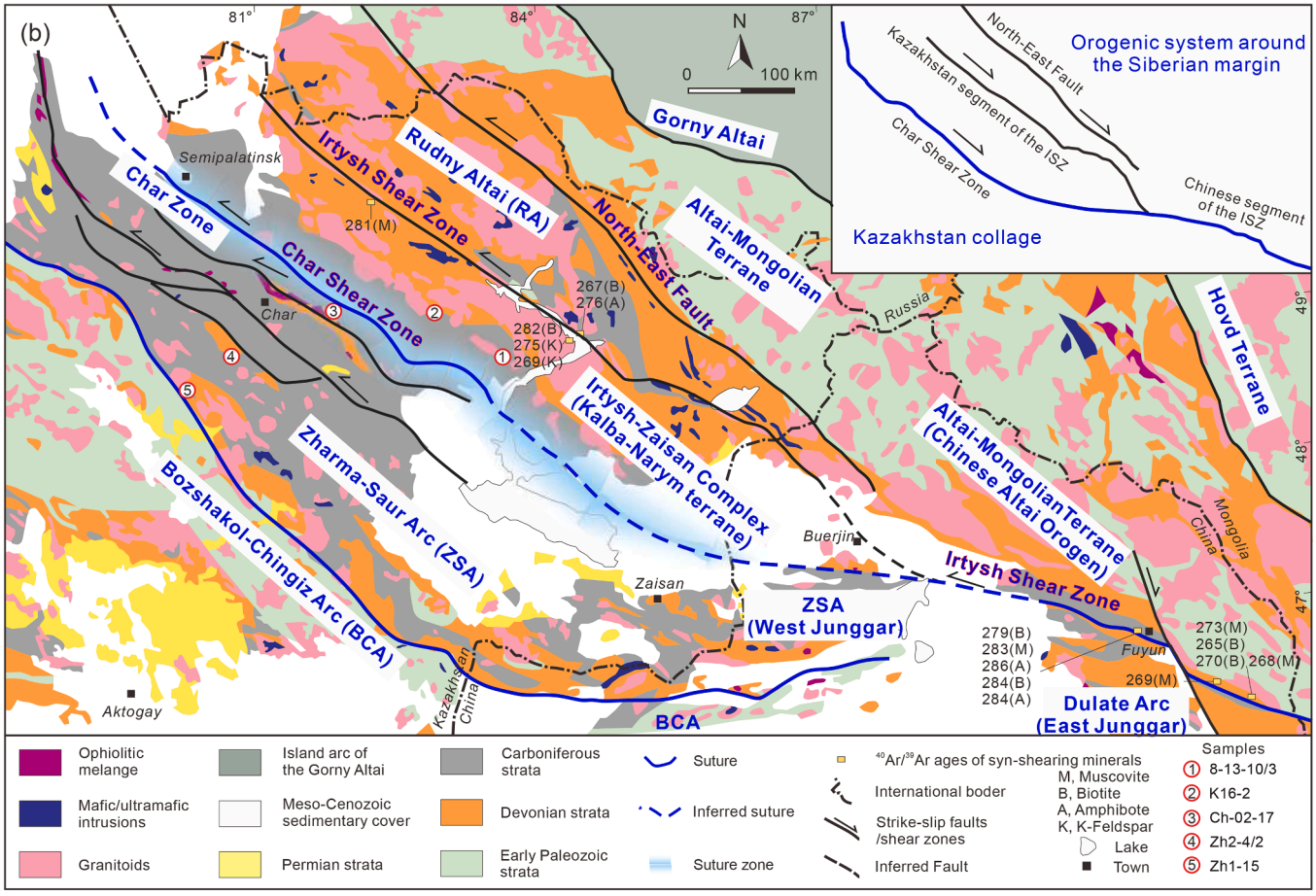

(caption on next page)

Fig. 1. (a) The tectonic map of the western CAOB (modified after Windley et al., 2007; Li et al., 2018; and Hu et al., 2020). The inset image shows the location of the CAOB (after Jahn, 2004). (b) A simplified geological map along the Irtysh-Char Shear Zone that marks the tectonic boundary of Siberian margin and the Kazakhstan collage (after Li et al., 2008). The inset figure highlights the major shear zones/faults along the collisional front of the Siberian margin and the Kazakhstan collage. Note that the Char Shear Zone that represents the tectonic boundary of the Siberian margin and the Kazakhstan collage in eatern Kazakhstan, merges into the Irtysh Shear Zone in NW China, where the Irtysh Shear Zone marks the bounday of the Siberian margin and the Kazakhstan collage. The $^{40}Ar/^{39}Ar$ ages of *syn*-shearing minerals along sinistral strike-slip shear zones are from Travin et al., 2001, Laurent-Charvet et al., 2003, Li et al., 2017, and Hu et al., 2020. Abbreviations, RA: Rudny Altai; IZC: Irtysh-Zaisan Complex; ZSA: Zharma-Saur Arc; BCA: Bozshakol-Chingiz Arc; BYA: Balkhash–Yili Arc; DVB: Devonian Volcanic Belt; NEF: North-East Fault; ISZ: Irtysh Shear Zone; CANTF: Chingiz-Alakol-North Tianshan Fault; MTSZ: Main Tianshan Shear Zone.

The NW-SE Char Shear Zone (also termed Gornostaev Shear Zone by Şengör et al., 1993) in eastern Kazakhstan has been interpreted to be a major suture zone within the CAOB, which represents the tectonic boundary between the orogenic system around the Siberian margin and the Kazakhstan collage (Fig. 1a; Buslov et al., 2001, 2004; Volkova et al., 2008; Safonova et al., 2012, 2018; Kuibida et al., 2016). It extends southeastward into NW China, where it is merged with the Irtysh Shear Zone (Fig. 1b; Laurent-Charvet et al., 2003; Li et al., 2017). Structurally, both Char and Irtysh shear zones show sinistral strike-slip kinematics (Buslov et al., 2003; Vladimirov et al., 2008; Li et al., 2015; Hu et al., 2020), which have been considered to result from the oblique convergence of the orogenic system around the Siberian margin and the Kazakhstan collage after the closure of the Ob-Zaisan Ocean (a branch of the Paleo-Asian Ocean that is also referred to as the Irtysh Ocean) (Qu and Zhang, 1991, 1994; Laurent-Charvet et al., 2003; Li et al., 2015, 2017; Hu et al., 2020). Available studies show that both the ocean plate stratigraphy (OPS) and arc-related fragments occur along the Char Shear Zone (Safonova et al., 2012, 2018, 2021). However, the initial collisional time of the two orogenic systems has been controversial. In eastern Kazakhstan, Glorie et al. (2012) proposed that the Ob-Zaisan Ocean was closed in the Early Carboniferous, on a basis of the interpreted *syn*-collisional origin of ~338 Ma intrusion. The subsequent geochemical studies for ~323–317 Ma igneous rocks by Kuibida et al. (2016) and Khromykh et al. (2019) also favor a *syn*-collisional origin for these rocks. In contrast, Zhang et al. (2020) proposed a subduction-related origin for 330–318 Ma igneous rocks to the north of the Char Shear Zone, indicating that the northward subduction of the Ob-Zaisan oceanic plate probably lasted until ~318 Ma. Such inconsistence shows the limitation of geochemical affinities of igneous rocks in tracing the tectonic transition associated with the closure of the oceanic basin. Farther southeast in NW China, detrital zircon data show that the Ob-Zaisan Ocean existed until the Late Carboniferous given that there is no exchange of detrital zircons for the orogenic system around the Siberian margin (Chinese Altai) and the Kazakhstan collage (West Junggar) in this period (Choulet et al., 2012a; Li et al., 2017; Song et al., 2020a). It remains enigmatic whether the Ob-Zaisan Ocean in NW China and eastern Kazakhstan share a similar tectonic history (e.g. synchronous/diachronous closure along the strike).

In this paper, we present new detrital zircon U–Pb and Hf isotope data from the Irtysh-Zaisan Complex, the Char Zone and the Zharma-Saur Arc in eastern Kazakhstan, with an aim to constrain the collisional time of the orogenic system around the Siberian margin and the Kazakhstan collage along the Char Shear Zone. Our results show that the Ob-Zaisan Ocean between the Siberian margin and the Kazakhstan collage in eastern Kazakhstan existed until ~321 Ma, similarly as the evolution of eastern segment of this oceanic basin in NW China.

2. Geological setting

The Char Shear Zone in eastern Kazakhstan marks the tectonic boundary of the orogenic system around the Siberian margin and the Kazakhstan collage (Fig. 1b; Buslov et al., 2001; Vladimirov et al., 2008; Volkova et al., 2008; Safonova et al., 2012; Kuibida et al., 2016; Safonova et al., 2018). The former was built by the accretion of a series of microcontinental blocks, island arcs, and accretionary complexes along the Siberian margin from Neoproterozoic to late Paleozoic (Wilhem et al., 2012; Xiao et al., 2015; Li et al., 2019), while the latter was predominantly developed via the amalgamation of microcontinental blocks (Kazakhstan microcontinent) and arc terranes in the early Paleozoic, followed by late Paleozoic oroclinal bending (Fig. 1a; Khain et al., 2003; Windley et al., 2007; Abrajevitch et al., 2008; Xiao et al., 2010; Degtyarev, 2011; Choulet et al., 2012b; Levashova et al., 2012; Rolland et al., 2013; Li et al., 2018). A ~100 km long ophiolitic belt (hosting OPS units) occurs within the collisional zone of the Siberian margin and the Kazakhstan collage (Char Zone; Fig. 1b), with high-pressure rocks (e.g. blueschist and eclogite that are metamorphosed from oceanic basalts) incorporated into the ophiolitic mélange (Buslov et al., 2001; Vladimirov et al., 2008; Volkova et al., 2008; Safonova et al., 2012, 2018).

2.1. Tectonic elements around the Siberian margin in eastern Kazakhstan

In eastern Kazakhstan, three ~NW-SE tectonic units of the Altai-Mongolian Terrane, the Rudny Altai, and the Irtysh-Zaisan Complex were developed along the Siberian margin (Fig. 1b). The northernmost unit of the Altai-Mongolian Terrane extends from eastern Kazakhstan, through NW China (Chinese Altai), to western Mongolia (Fig. 1b), and it mainly comprises early Paleozoic *meta*-sedimentary/volcanic rocks (Buslov et al., 2001; Badarch et al., 2002; Windley et al., 2002; Cai et al., 2011a). This terrane has been interpreted to be an accretionary complex (Long et al., 2008, 2012; Jiang et al., 2012; Chen et al., 2014, 2015), which together with the coeval magmatic arc (Ikh-Mongol arc) in western Mongolia constitutes an Andean-type subduction system along the Siberian margin (Bold et al., 2016; Soejono et al., 2017; Janousek et al., 2018; Li et al., 2019). The Altai-Mongolian Terrane is bounded with the Rudny Altai farther south by a sinistral strike-slip fault of the North-East Fault (Fig. 1b). The Rudny Altai has been interpreted to be a back-/intra-arc extensional basin that was developed along the southern margin of the Altai-Mongolian Terrane (Buslov et al., 2004; Lobanov et al., 2014; Kuibida et al., 2020). The oldest rocks in the Rudny Altai are Silurian to Devonian *meta*-sedimentary rocks (metasandstones, schists, and phyllites), which are overlain by Devonian to Carboniferous rhyolite-basalt lava, volcanic breccia, tuff, conglomerate, sandstone and minor limestone (Buslov et al., 2001; Buslov et al., 2004; Kruk et al., 2011; Lobanov et al., 2014). Farther south, the Irtysh-Zaisan Complex (also termed the Kalba-Narym terrane, Buslov et al., 2001) is separated from the Rudny Altai by the Irtysh Shear Zone (Şengör et al., 1993; Buslov et al., 2004; Glorie et al., 2012). The Irtysh-Zaisan Complex contains migmatite, amphibolite, gneiss, schist, metasandstone, quartzite, marble, as well as a small amount of metamorphosed basalt and chert (Şengör et al., 1993; Buslov et al., 2004; Briggs et al., 2007; Chen et al., 2019). Its counterpart in NW China, has been interpreted as a Devonian to Carboniferous accretionary complex consisting of oceanic plate stratigraphy and continent-marginal sedimentary rocks (O'Hara et al., 1997; Briggs et al., 2007; Li et al., 2015, 2017; Xiao et al., 2015; Chen et al., 2019).

The Altai-Mongolian Terrane, the Rudny Altai, and the Irtysh-Zaisan Complex in eastern Kazakhstan are voluminously intruded by late Paleozoic granitoids (Fig. 1b; Glorie et al., 2012; Khromykh et al., 2016; Kuibida et al., 2019, 2020; Zhang et al., 2020; Kotler et al., 2021). The Devonian to Carboniferous magmatism was considered to be associated with the northward subduction of the Ob-Zaisan oceanic plate (Buslov et al., 2004; Safonova, 2014; Kuibida et al., 2020; Zhang et al., 2020), while the Permian intrusions were likely related to the collision of the

Siberian margin and the Kazakhstan collage (Vladimirov et al., 2008; Kuibida et al., 2009, 2019).

2.2. Island arcs of the Kazakhstan collage in eastern Kazakhstan

The Kazakhstan collage shows a U-shaped geometry in a map view (Kazakhstan Orocline; Şengör et al., 1993), which is delineated by two curved magmatic arc systems of the Devonian Volcanic Belt and the Late Devonian to Carboniferous Balkhash–Yili Arc (Fig. 1a; Levashova et al., 2003, 2012; Windley et al., 2007; Abrajevitch et al., 2008; Degtyarev, 2011; Bazhenov et al., 2012; Li et al., 2018). Along the northern limb of the orocline, both arc systems were developed over an early Paleozoic island arc of the Bozshakol-Chingiz Arc (Fig. 1a) that mainly contains Cambrian to Silurian mafic to felsic volcanic rocks, pyroclastic rocks, and chert (Feng et al., 1989; Degtyarev and Ryazantsev, 2007; Chen et al., 2010; Shen et al., 2015), and Late Silurian to Carboniferous volcanic rocks and carbonate (Degtyarev and Ryazantsev, 2007; Wei et al., 2009). The late Paleozoic intra-oceanic island arc of the Zharma-Saur Arc occurs to the north of the Bozshakol-Chingiz Arc (Fig. 1a; Safonova et al., 2017). It is dominated by Devonian to Carboniferous volcanic rocks, limestone and clastic rocks (Zhu and Xu, 2006; Vladimirov et al., 2008; Chen et al., 2010), which are intruded by late Paleozoic mafic to felsic plutons (Han et al., 2006; Vladimirov et al., 2008; Zhou et al., 2008; Chen et al., 2010; Zhang et al., 2015a; Liu et al., 2018). Farther north, the Char Zone is dominated by mafic to andesitic volcanic rocks, tuff and sandstone, which is mixed with the ophiolitic mélange and is affected by a series of sinistral strike-slip faults (Char Shear Zone; Fig. 1b). The volcanic rocks within the Char Zone show Late Devonian to Early Carboniferous zircon U–Pb ages and positive $\varepsilon_{Nd}(t)$ values (3–9) (Safonova et al., 2018). The greywackes of the Char Zone are characterized by Carboniferous detrital zircon age peaks, positive zircon $\varepsilon_{Hf}(t)$ values (mostly in the range of 5 to 14) and whole-rock $\varepsilon_{Nd}(t)$ values (5–8) (Safonova et al., 2021).

3. Zircon U–Pb geochronology and Hf isotope analysis

3.1. Sample description

Five samples were collected for detrital zircon U–Pb dating and Hf isotope analysis with an aim to constrain the provenance variation across the Char Shear Zone in eastern Kazakhstan. All sample locations are illustrated in Fig. 1b. Two samples (8–13-10/3 and K16-2; Fig. 1b) are from the Irtysh-Zaisan Complex to the north of the Char Shear Zone. Sample 8–13-10/3 (GPS coordinate: 49°06′11.11′′ N, 83°20′22.15′′ E) is a medium-grained sandstone with oriented lens-shaped quartz and feldspar to define a foliation (Fig. 2a). The other sample from the Irtysh-Zaisan Complex (K16-2; GPS coordinate: 49°30′47.40′′ N, 82°48′15.00′′ E) is a mica quartz schist, with a mineral assemblage of quartz, muscovite and minor biotite (Fig. 2b).

Two samples (Zh2-4/2 and Zh1-15; Fig. 1b) were collected from

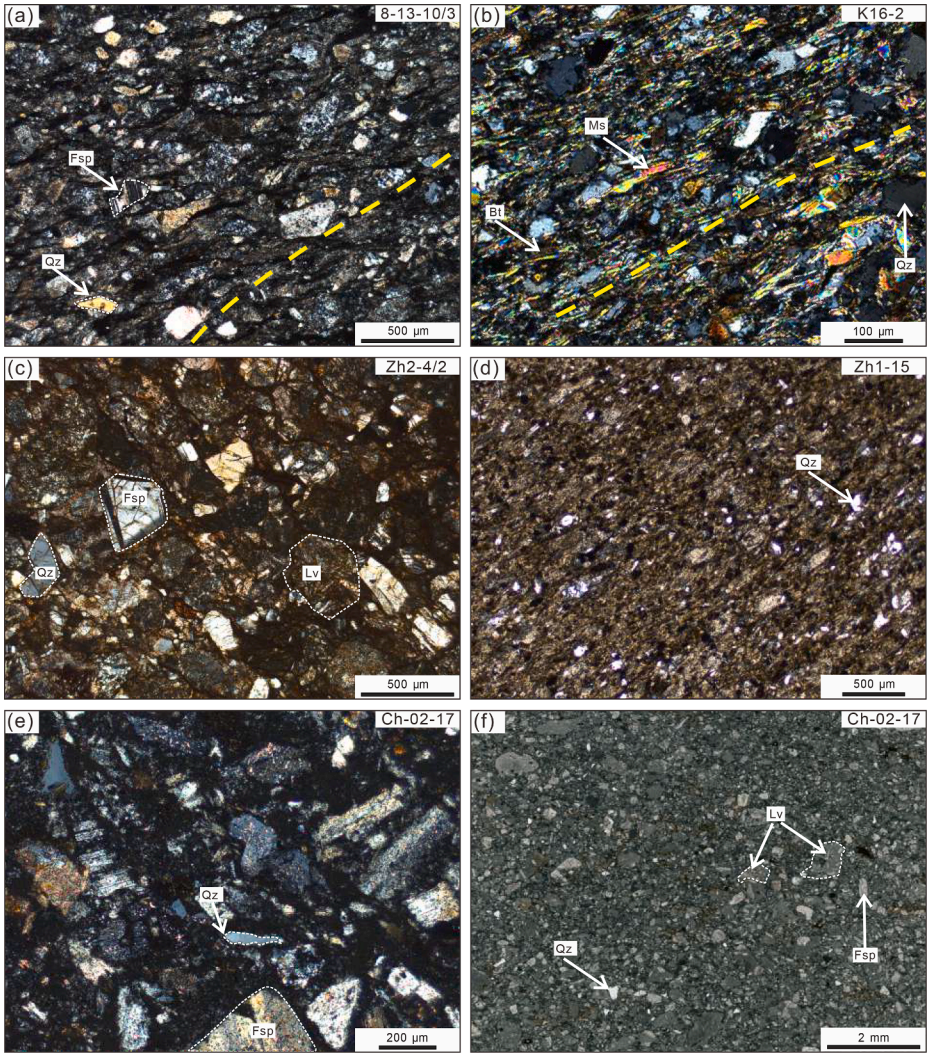

Fig. 2. Photographs of samples for zircon U–Pb Hf isotope analysis. (a) Medium-grained sandstone from the Irtysh-Zaisan Complex, with a secondary foliation indicated by yellow dashed line. (b) Mica quartz schist from the Irtysh-Zaisan Complex, with preferred alignment of muscovite and biotite to define a foliation (yellow dashed line). (c) Medium-grained sandstone from the Zharma-Saur Arc, which contains quartz, feldspar, and minor calcite and volcanic lithic fragments. (d) Siltstone from the Zharma-Saur Arc, which is mainly composed of quartz, feldspar, and opaque minerals. (e–f) Fine-grained sandstone, which was collected along the Char Zone, containing feldspar, volcanic lithic fragments, and minor quartz and opaque minerals. Abbreviations, Qz: quartz; Fsp: feldspar; Ms: muscovite; Bt: biotite; Lv: volcanic lithic fragment. (For interpretation of the references to colour in this figure legend, the reader is referred to the web version of this article.)

Carboniferous strata of the Zharma-Saur Arc. Sample Zh2-4/2 (GPS coordinate: 49°13′46.09′′ N, 80°45′40.08′′ E) is a medium-grained sandstone that contains quartz, feldspar, and minor calcite and volcanic lithic fragments (Fig. 2c), while sample Zh1-15 (GPS coordinate: 48°56′54.07′′ N, 80°14′15.03′′ E) is a moderately sorted siltstone that is composed of quartz, felspar, and opaque minerals (Fig. 2d).

One additional sample (Ch-02–17; GPS coordinate: 49°35′07.00′′ N, 81°52′44.04′′ E) was taken along the northeastern flank of the Char Zone (Fig. 1b). It is a fine-grained sandstone that is composed of subangular feldspar, volcanic lithic fragments, quartz, and opaque minerals (Fig. 2e, f).

3.2. Methods

Zircon grains were extracted using traditional heavy liquid and magnetic techniques, and were mounted in an epoxy resin. Cathodoluminescence (CL) images were taken in order to unravel the internal structure of zircons. Zircon U–Pb dating was conducted by laser ablation inductively coupled plasma mass spectrometry (LA-ICP-MS) (Resonetics RESOlution S-155 laser + Agilent 7900) at the Guangzhou Institute of Geochemistry, Chinese Academy of Sciences (GIG-CAS). For detailed operating conditions and analytical procedures, see Li et al. (2012). The laser diameter was set as 29 μm for samples 8–13-10/3, K16-2, and Zh2-4/2, and 19 μm for samples Zh1-15 and Ch-02–17. The frequency of the laser was 6 Hz. Zircon 91500 was used as external standards. The content of trace elements in zircon was quantitatively

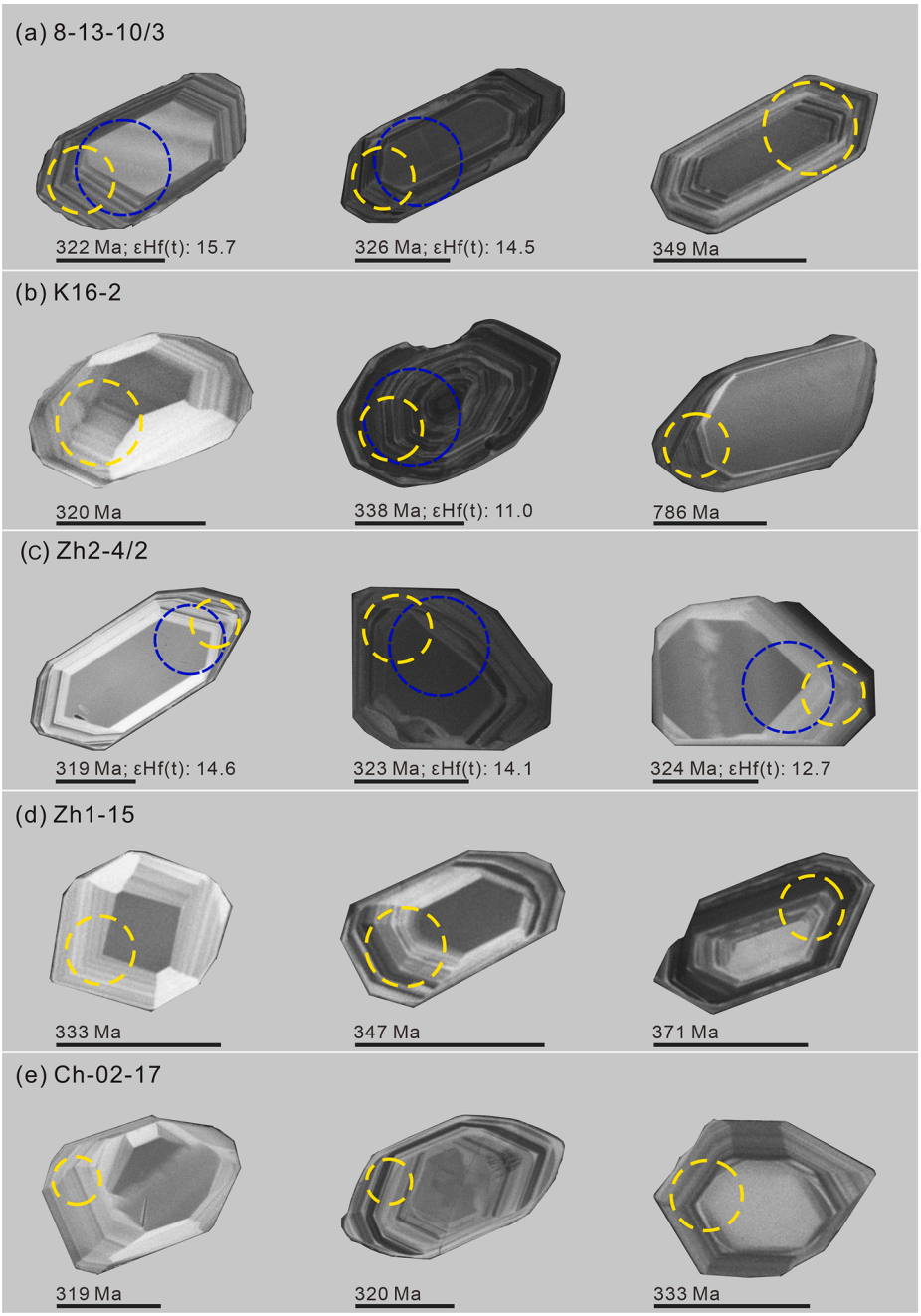

Fig. 3. Representative CL images of analyzed zircon grains, in which U–Pb ages and $\varepsilon_{Hf}(t)$ values are illustrated. Analyzed spots for U–Pb dating and Hf isotope analysis are indicated by yellow and blue circles, respectively. The black line below each zircon image is for scale (50 μm). (For interpretation of the references to colour in this figure legend, the reader is referred to the web version of this article.)

analyzed with NIST610 as an external calibration reference and Si as an internal standard. The first 20 s was set to detect the gas blank, followed by 50 s laser ablation for each spot signal. The ICPMSDataCal 10.8 and the Isoplot 4.15 were used for performing off-line analyzed signals and calculating ages, respectively (Ludwig, 2003; Liu et al., 2008; Lin et al., 2016).

Hf-in-zircon isotopic analyses of three samples (8–13-10/3, K16-2, and Zh2-4/2) were conducted at the GIG-CAS via using a Neptune Plus MC-ICP-MS (Thermo Scientific), coupled with a RESOlution M−50 193 nm laser ablation system (Resonetics). Detailed operating conditions and analytical methods are descripted in Zhang et al. (2014). In order to improve the instrumental sensitivity, an X skimmer cone was designed in the interface. The single spot size and frequency of the laser were 45 μm and 6 Hz. All isotope signals were detected with Faraday cups under static mode. Each analysis for zircons includes 20 s background signal and 30 s data signal. Isobaric interference of ^{176}Yb and ^{176}Lu on ^{176}Hf was corrected by ^{173}Yb and ^{175}Lu. The corrected natural ratio values of ^{176}Yb/^{173}Yb and ^{176}Lu/^{175}Lu, are 0.79381 (Segal et al., 2003) and 0.02656 (Wu et al., 2006), respectively. The mass bias factor of Lu is assumed to be the same as that of Yb, which is calculated from the measured ^{173}Yb/^{171}Yb and the natural ratio of 1.13268 (Chu et al., 2002). The mass bias of ^{176}Hf/^{177}Hf was normalized to ^{179}Hf/^{177}Hf = 0.7325 with an exponential law. The detailed data reduction procedure is documented in Zhang et al. (2015b). Nineteen Plešovice zircon yielded a weighted mean of ^{176}Hf/^{177}Hf = 0.282486 ± 0.000008 (2SD), which is consistent within errors with reported in Sláma et al. (2008).

3.3. Results

Representative CL images of analyzed zircons are shown in Fig. 3. The U–Pb and Hf isotope data of zircons are presented in Supplementary Tables 1 and 2. ^{207}Pb/^{206}Pb ages are used for zircons older than 1000 Ma, and ^{206}Pb/^{238}U ages are used for zircons younger than 1000 Ma. The values of $\varepsilon_{Hf}(t)$ were calculated using ^{176}Lu/^{177}Hf = 0.0332 and ^{176}Hf/^{177}Hf = 0.282772 (Blichert-Toft and Albarede, 1997). The depleted mantle line, exhibited in Fig. 5 is based on the present ^{176}Hf/^{177}Hf = 0.28325 and ^{176}Lu/^{177}Hf = 0.0384 (Griffin et al., 2000).

Detrital zircons from samples 8–13-10/3 and K16-2 within the Irtysh-Zaisan Complex, are predominantly prismatic with variable luminescence in CL images (Fig. 3a, b). Most zircons are 30–200 μm long, and are characterized by oscillatory zoning, which together with Th/U ratio range from 0.22 to 2.96, implying an igneous origin (Supplementary Table 1). One additional zircon grain has a low Th/U ratio (0.06), but it is characterized by oscillatory zoning, indicating a magmatic origin (e.g. Gebauer, 1996; Wu and Zheng, 2004). Total 65 zircon grains were analyzed for sample 8–13-10/3. 61 zircons yield concordant early Paleozoic ages from 313 to 536 Ma, with a major age peak (~330 Ma) and three minor age peaks (~348 Ma, ~376 Ma, and ~473 Ma; Fig. 4a, b). The Hf isotope analysis for this group of zircons gives $\varepsilon_{Hf}(t)$ values ranging from −1.6 to 19.3 (Fig. 5a). Additional 3 analyses give scattering Precambrian ages of 554 Ma, 675 Ma, and 835 Ma. As for sample K16-2, 56 zircon grains yield Paleozoic U-Pb ages (317–533 Ma) with a remarkable age peak at ~328 Ma and two minor age peaks of ~452 Ma and ~488 Ma. These Paleozoic zircons have predominant $\varepsilon_{Hf}(t)$ values from −6.3 to 20.1 except one 325 Ma zircon grain with −14.8 $\varepsilon_{Hf}(t)$ value. Additional 4 zircons give Precambrian ages of 619 Ma, 786 Ma, 942 Ma, and 2028 Ma (Fig. 4c, d).

Detrital zircons from samples Zh2-4/2 and Zh1-15 in the Zharma-Saur Arc are euhedral or slightly round, and are commonly 30–150 μm long (Fig. 3c, d). CL images of these zircon grains display that they have mostly oscillatory zoning, which together with the evidence of moderate luminescence and Th/U ratios (0.31–0.95, Supplementary Table 1), indicates their magmatic origin. Sample Zh2-4/2 is characterized by a major zircon age population of 306–354 Ma, with a major peak at ~325 Ma (Fig. 4e, f), and $\varepsilon_{Hf}(t)$ values of these zircons are in a narrow range of 10.3 to 16.5 (Fig. 5b). Additional two zircon grains yield relatively young ages of 291 Ma and 297 Ma. These Permian ages are younger than the Carboniferous deposition age of analyzed samples, and we consider that their U–Pb system may have been disturbed subsequently. Zircon grains from sample Zh1-15 give U–Pb ages from 332 Ma to 371 Ma, with a prominent peak at ~338 Ma (Fig. 4g, h).

Sample Ch-02–17 from the Char Zone contains stubby to prismatic zircons with low to high luminescence and relatively small sizes (40–100 μm long, Fig. 3e). They exhibit clear oscillatory zoning with relatively high Th/U ratios of 0.21–1.32 (Supplementary Table 1), indicating an igneous origin. 47 zircon grains from this sample give U-Pb ages in a narrow age range of 312–376 Ma, peaked at ~321 Ma and ~340 Ma (Fig. 4i, j). Additional one grain yields a Silurian age of 431 Ma.

4. Discussion

The closure of the Ob-Zaisan Ocean and the related arc amalgamation are imperative for the tectonic reconstruction of the western CAOB. Our five samples for detrital zircon dating and Hf isotope analysis across the Char Shear Zone have significant implications for the location and time of the closure of the Ob-Zaisan Ocean.

4.1. Provenance of detrital zircons

Two Carboniferous samples (8–13-10/3 and K16-2) of the Irtysh-Zaisan Complex to the north of the Char Shear Zone show similar detrital zircon populations, and both are dominated by Devonian to Carboniferous detrital zircon ages (Fig. 4b, d). Combining detrital zircons from these two samples, total 124 analyses define four major age peaks of ~328 Ma, ~347 Ma, ~374 Ma and ~487 Ma (Fig. 6a), and have a broad $\varepsilon_{Hf}(t)$ range of –6.3–20.1, similar as ages and $\varepsilon_{Hf}(t)$ values of detrital zircons from the Chinese segment of the Irtysh-Zaisan Complex (Figs. 6c and 7a; Li et al., 2015, 2017, 2019; Song et al., 2020b). Devonian to Carboniferous volcanic rocks widely occur within the Rudny Altai (Saraev et al., 2012; Lobanov et al., 2014; Kuibida et al., 2020), and ~338–318 Ma granitic rocks have been recognized along the Rudny Altai (Glorie et al., 2012; Kuibida et al., 2013; Kruk et al., 2014; Zhang et al., 2020). These igneous rocks likely represent major source of Devonian to Carboniferous detrital zircons in the Irtysh-Zaisan Complex. In addition, ~445–353 Ma plutonic rocks widely intrude into the Chinese segment of the Altai-Mongolian Terrane (Fig. 1b; Wang et al., 2006; Yuan et al., 2007; Sun et al., 2009; Wang et al., 2010; Cai et al., 2011b; Yang et al., 2011; Wang et al., 2011; Tong et al., 2012; Yu et al., 2017), and may also contribute to the provenance of Devonian to Early Carboniferous detrital zircons in the Irtysh-Zaisan Complex. Early Paleozoic detrital zircons with the peak age of ~487 Ma and Precambrian detrital zircons (554 Ma, 619 Ma, 675 Ma, 786 Ma, 835 Ma, 942 Ma, and 2028 Ma) in the Irtysh-Zaisan Complex, overlap in time with detrital zircon populations of early Paleozoic clastic rocks from the Altai-Mongolian Terrane (Fig. 6e; Long et al., 2007), indicating that these detrital zircons may recycle from the Altai-Mongolian Terrane.

Two Carboniferous samples (Zh2-4/2 and Zh1-15) from the Zharma-Saur Arc to the south of the Char Shear Zone are dominated by Devonian to Carboniferous detrital zircon grains (Fig. 4f, h). Total 98 analyses from these two samples yield a major age peak at ~335 Ma (Fig. 6b), which is compatible with detrital zircon ages of the Zharma-Saur Arc in the West Junggar of NW China (Fig. 6d; Li et al., 2017). Devonian to Carboniferous arc-related magmatism is widespread within the Zharma-Saur Arc (Han et al., 2006; Zhou et al., 2008, 2015; Chen et al., 2010; Choulet et al., 2012a; Yang et al., 2014; Liu et al., 2018), and we consider that these magmatic rocks are the major source of Devonian to Carboniferous detrital zircons. In addition, $\varepsilon_{Hf}(t)$ of detrital zircons from sample Zh2-4/2 is characterized by positive values of 10–19 (Fig. 5b), which is consistent with the range of $\varepsilon_{Hf}(t)$ values from coeval detrital zircons in West Junggar (NW China; Fig. 7b; Li et al., 2017), suggesting juvenile origin of the coeval magmatism in the whole Zharma-Saur Arc.

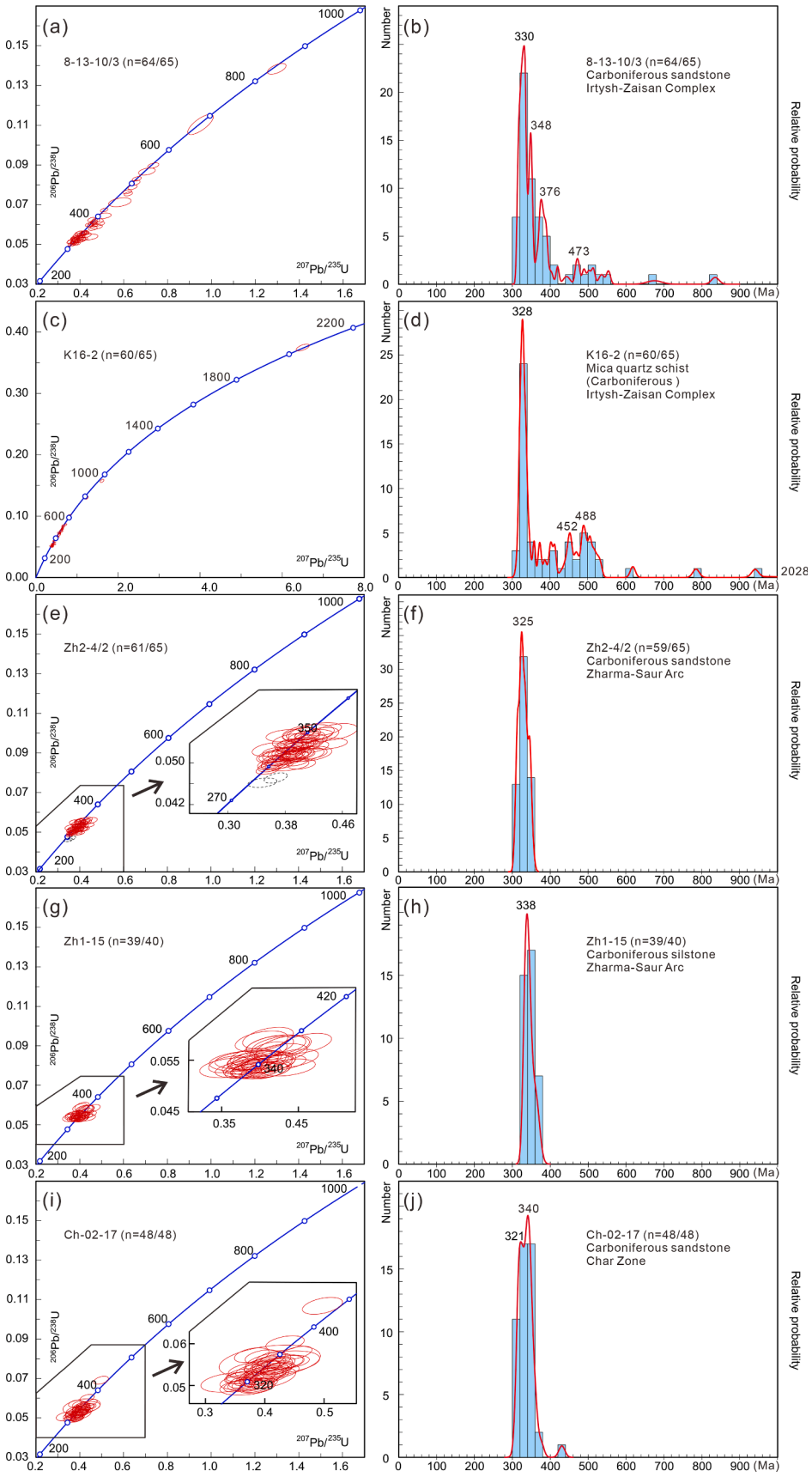

Fig. 4. U–Pb concordia plots (left) and age probability diagrams (right) of detrital zircons. The error is 1σ level indicated by ellipses.

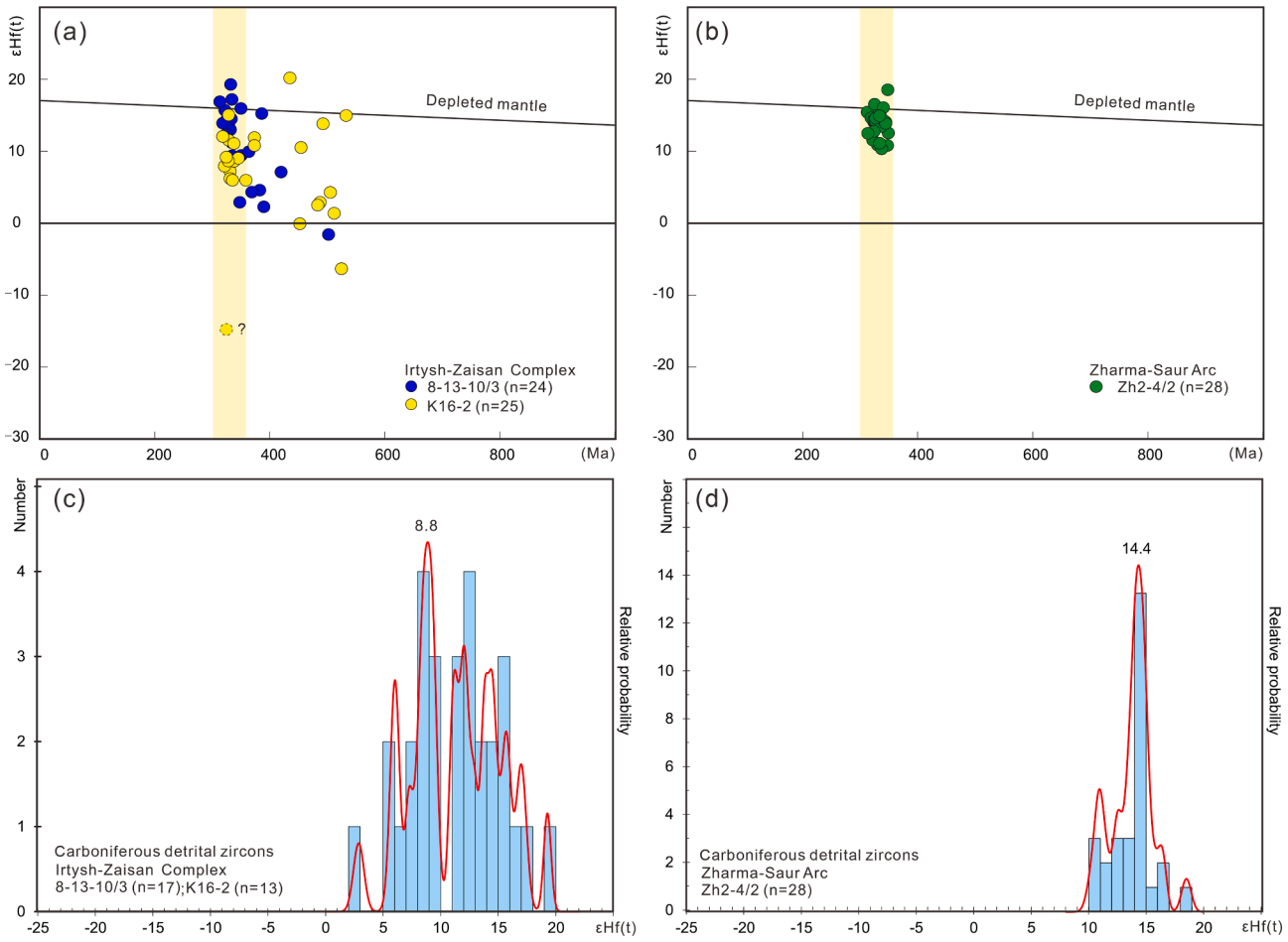

Fig. 5. (a-b) Diagram of $\varepsilon_{Hf}(t)$ values versus crystallizing ages for detrital zircons in this study. (c-d) Probability diagrams of $\varepsilon_{Hf}(t)$ values of Carboniferous detrital zircons.

An additional sample (Ch-02–17) was collected along the Char Zone. Available structural work demonstrates that a series of narrow sinistral faults characterize the Char Zone (Fig. 1b; Vladimirov et al., 2008), and therefore rocks from the Char Zone may have been transported horizontally in response to strike-slip movement. Our results show a major Devonian to Carboniferous detrital zircon population for sample Ch-02–17 (Fig. 4j), which is comparable to two samples from the Zharma-Saur Arc (Fig. 6b, f). A Silurian zircon grain (~431 Ma) from this sample overlaps within error with ~428 Ma andesite in the Zharma-Saur Arc (Zhang et al., 2015a), indicating that ~431 Ma detrital zircon grain may source from the Silurian magmatism within the Zharma-Saur Arc. Such data sets are consistent with the recent studies that show similar detrital zircon age populations of Carboniferous sedimentary rocks from the Char Zone as coeval clastic rocks in the Zharma-Saur Arc (Choulet et al., 2012a; Li et al., 2017; Safonova et al., 2021; Song et al., 2020a), which seems to indicate that clastic rocks within the Char Zone may tectonically belong to the Zharma-Saur Arc.

4.2. Tectonic implications

4.2.1. The tectonic boundary of the orogenic system around the Siberian margin and the Kazakhstan collage in eastern Kazakhstan

Our results show various provenances of sedimentary rocks across the Char Shear Zone. This supports the previous idea that the Char Shear Zone represents the tectonic boundary between the orogenic system around the Siberian margin and the Kazakhstan collage (Fig. 1b; Şengör et al., 1993; Travin et al., 2001; Buslov et al., 2004; Vladimirov et al., 2008; Glorie et al., 2012). The Carboniferous sedimentary rocks (samples 8–13-10/3 and K16-2) from the Irtysh-Zaisan Complex (the Kazakhstan segment) to the northeast of the Char Shear Zone, contain abundant pre-Devonian detrital zircons peaked at ~488 Ma (Fig. 6a), similar to the detrital zircon populations from the Chinese segment of the Irtysh-Zaisan Complex (Fig. 6c; Li et al., 2015, 2017, 2019; Song et al., 2020b). On the contrary, the Carboniferous clastic rocks (sample Zh1-15 and Zh2-4/2) from the Zharma-Saur Arc to the southwest of the Char Shear Zone, are dominated by Devonian to Carboniferous detrital zircons that show a major age peak at ~335 Ma (Fig. 6b), which is consistent with the detrital zircon ages from the Zharma-Saur Arc in the West Junngar (NW China) (Fig. 6d; Choulet et al., 2012a; Li et al., 2017; Song et al., 2020a). In addition, the Carboniferous detrital zircons from the Zharma-Saur Arc have a narrow range of $\varepsilon_{Hf}(t)$ values (around 10–19, Fig. 5c), which is distinct from the coeval detrital zircons from the Irtysh-Zaisan Complex that exhibit a relatively broad range (about 4–19, Fig. 5d), indicating different sources of the Carboniferous detrital zircons in the Zharma-Saur Arc and the Irtysh-Zaisan Complex.

On a larger scale, the Char Shear Zone extends into NW China, where it is merged with the Irtysh Shear Zone (Fig. 1b), with the latter representing the tectonic boundary of the Siberian margin (Chinese Altai) and the Kazakhstan collage (West Junggar) in NW China (Qu and Zhang, 1991, 1994; Li et al., 2017). Ophiolitic rocks have been recognized along both the Chinese segment of the Irtysh Shear Zone and the Char Shear Zone in eastern Kazakhstan (Buslov et al., 2001; Vladimirov et al., 2008; Volkova et al., 2008; Safonova et al., 2012, 2018; Wang et al., 2012; Song et al., 2020b), which together with ~444–429 Ma blueschists and eclogites within these shear zones (Buslov et al., 2001; Volkova et al., 2008) supports the interpretation with the Irtysh-Char Shear Zone as a

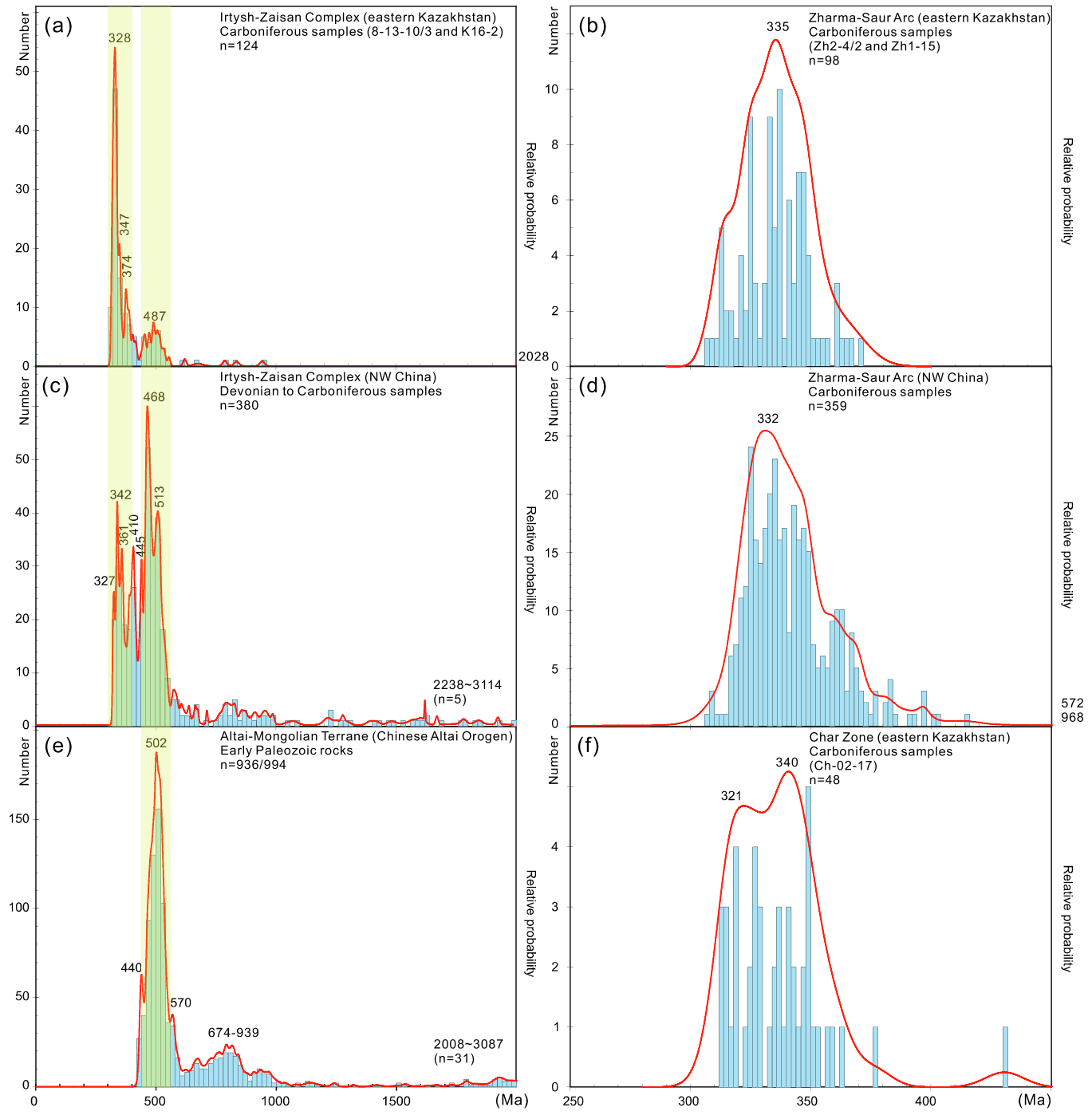

Fig. 6. (a-b) Age probability diagrams of all detrital zircon grains from the Irtysh-Zaisan Complex and the Zharma-Saur Arc in eastern Kazakhstan. (c-d) Age probability diagrams of detrital zircon grains from the Chinese segment of the the Irtysh-Zaisan Complex (Li et al., 2015, 2017, 2019; Song et al., 2020b) and the Zharma-Saur Arc in the West Junggar of NW China (Choulet et al., 2012a; Li et al., 2017; Song et al., 2020a). (e) Age probability diagrams of detrital zircons from early Paleozoic rocks of the Chinese Altai Orogen (Li et al., 2019 and reference therein). (f) Age probability diagrams of detrital zircons from the Char Zone.

major suture zone of the Siberian margin and the Kazakhstan collage.

4.2.2. The collision of the Siberian margin and Kazakhstan collage in eastern Kazakhstan

The collisional front of the Siberian margin and the Kazakhstan collage is represented by the Irtysh-Zaisan Complex and the Zharma-Saur Arc/Char Zone (Fig. 1a). Buslov et al., (2004) considered that the Irtysh-Zaisan Complex in eastern Kazakhstan was probably deposited in a passive margin setting. However, the recent work along the Chinese segment of the Irtysh-Zaisan Complex suggests that it was probably developed within a late Paleozoic accretionary wedge given the mixed occurrence of oceanic plate stratigraphy with continent-marginal clastic rocks (Briggs et al., 2007; Li et al., 2015, 2017; Xiao et al., 2015; Chen et al., 2019). Two Carboniferous samples (samples 8–13-10/3 and K16-2) from the Irtysh-Zaisan Complex in eastern Kazakhstan are characterized by abundant Carboniferous detrital zircons. These ages are close to the deposition time of the analyzed samples and are consistent with a convergent setting pattern on a cumulative probability plot (Fig. 8), thus supporting an accretionary wedge origin of the Irtysh-Zaisan Complex. The late Paleozoic arc-related magmatism was widely recognized within

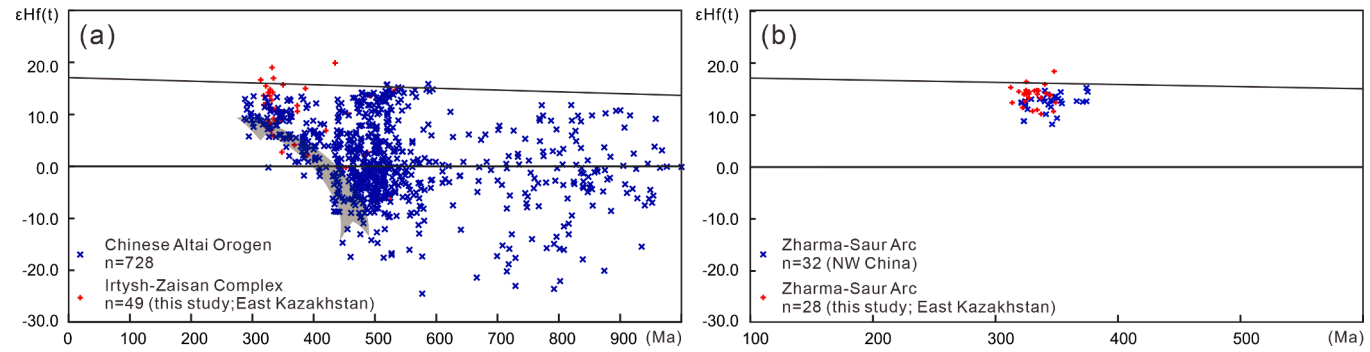

Fig. 7. (a) Diagram of $\varepsilon_{Hf}(t)$values versus crystallizing ages for detrital zircons from the Chinese Altai Orogen in NW China and the Irtysh-Zaisan Complex in eastern Kazakhstan (Li et al., 2019 and reference therein). The evolution of $\varepsilon_{Hf}(t)$ towards positive values after ~400 Ma was interprted to represent an episode of trench retreat (Li et al., 2019). (b) Diagram of $\varepsilon_{Hf}(t)$ values versus crystallizing ages for detrital zircons from the Zharma-Saur Arc in eastern Kazakhstan and NW China (West Junggar) (Li et al., 2017).

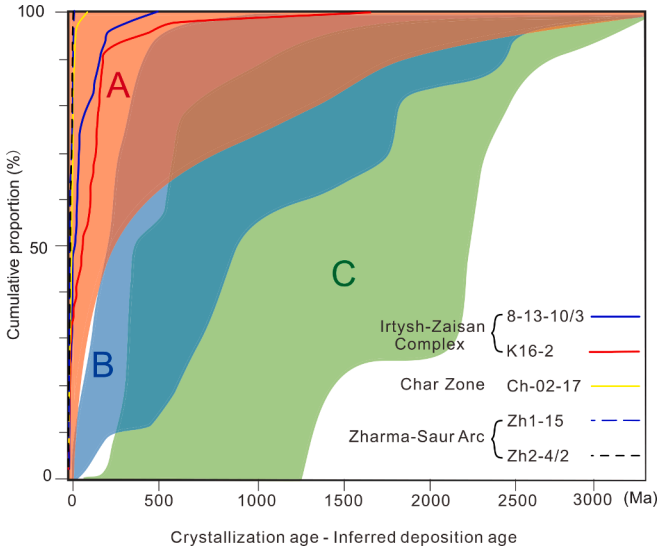

Fig. 8. Cumulative proportion curves for the difference of the crystallization age of detrital zircons with the depositional age of sedimentary rocks (Crystallization age-inferred deposition age). The plot of the general fields for convergent (A), collisional (B), and extensional (C) tectonic settings is based on Cawood et al. (2012).

the Rudny Aitai and Altai-Mongolian Terrane farther north (Vladimirov et al., 2008; Chai et al., 2009; Wan et al., 2010; Wang et al., 2011; Cai et al., 2012a; Kuibida et al., 2019; Zhang et al., 2020). The coeval development of magmatic arc and the Irtysh-Zaisan accretionary complex suggests a late Paleozoic arc-trench subduction system around the Siberian margin, associated with the northward subduction of the Ob-Zaisan oceanic plate. In addition, Carboniferous sedimentary rocks (samples Zh1-15 and Zh2-4/2) of the Zharma-Saur Arc are dominated by Devonian to Carboniferous detrital zircon grains (Fig. 4f, h) and exhibit a convergent setting pattern on a cumulative probability plot (Fig. 8), which is consistent with the previous interpretation that the Zharma-Saur Arc was developed in an intra-oceanic arc setting (Chen et al., 2017). Buslov et al. (2001) and Choulet et al. (2015) considered that the Zharma-Saur Arc was developed via southward subduction over the Bozshakol-Chingiz Arc (Fig. 1a). This interpretation is not preferred given the lack of Ordovician detrital zircons in the Zharma-Saur arc (Fig. 1b), which widely occurs within the Bozshakol-Chingiz Arc (Choulet et al., 2012a; Song et al., 2020a). Alternatively, the Zharma-Saur Arc may represent an independent late Paleozoic intra-oceanic arc (Safonova et al., 2017, 2021) separated from the Bozshakol-Chingiz Arc by an oceanic basin.

The collisional time of the Siberian margin and the Kazakhstan collage in eastern Kazakhstan can be constrained by our detrital zircon data. Our results demonstrate the absence of pre-Devonian detrital zircon grains within the Carboniferous strata of the Zharma-Saur Arc and the Char Zone, but such zircons widely exit within the Irtysh-Zaisan Complex (Section 4.1). This indicates that the Carboniferous strata of the Zharma-Saur Arc and the Char Zone did not receive detrital zircons from the orogenic system around the Siberian margin, and the Ob-Zaisan Ocean still bounded the Siberian margin with the Kazakhstan collage during the deposition of the Carboniferous strata of the Zharma-Saur Arc and the Char Zone. Three samples of Zh2-4/2, Zh1-15, and Ch-02–17 from the Zharma-Saur Arc and the Char Zone give the youngest age peaks of ~325 Ma, ~338 Ma, ~321 Ma, respectively. We consider that the youngest detrital zircon age peak of ~321 Ma from sample Ch-02–17 (Fig. 4j) within the Carboniferous strata of the Char Zone can give a maximum time constraint for the closure of the Ob-Zaisan Ocean. This timing constraint is compatible with the detrital zircon age data from NW China (West Junngar), which suggest that the Ob-Zaisan Ocean in NW China was closed after ~323 Ma (Li et al., 2017).

The youngest constraint for the closure of the Ob-Zaisan Ocean in eastern Kazakhstan can be determined by the activity time of the sinistral Char Shear Zone. This shear zone represents the tectonic boundary of the Siberian margin and the Kazakhstan collage in eastern Kazakhstan, and both systems must be collided prior to the sinistral shearing. The direct dating of the Char Shear Zone has not been undertaken till now, but this shear zone merges into the Irtysh Shear Zone in NW China. Therefore, both Char and Irtysh shear zones were supposed to be active simultaneously. The $^{40}Ar/^{39}Ar$ dating on *syn*-shearing minerals along the Irtysh Shear Zone constrains an age range of ~286–265 Ma for the sinistral strike-slip deformation (Fig. 1b; Travin et al., 2001; Laurent-Charvet et al., 2003; Buslov et al., 2004; Zhang et al., 2012; Li et al., 2017; Hu et al., 2020), which together with our detrital zircon data suggests that the closure of the Ob-Zaisan Ocean in eastern Kazakhstan occurred within a period of ~321–286 Ma, similarly as the closure of this oceanic basin in NW China (Li et al., 2015, 2017; Hu et al., 2020).

The development of a series of sinistral strike-slip shear zones (Char, Irtysh and North-East shear zones/faults) along the tectonic boundary of the Siberian margin and the Kazakhstan collage in the Permian suggests the oblique convergence of the both systems in this period (Fig. 9; Qu and Zhang, 1994; Buslov et al., 2003, 2004; Vladimirov et al., 2008; Kuibida et al., 2019). Li et al. (2015, 2017) and Hu et al. (2020) recognized early Permian sub-horizontal foliations and related ~NW-SE orogen-parallel stretching lineations along the southern Chinese Altai Orogen (the southernmost segment of the *peri*-Siberian system in NW China), and suggested an episodic orogen-parallel extensional event prior to the oblique convergence, but post to the initial closure of the Ob-Zaisan Ocean. It remains enigmatic whether such earlier crustal

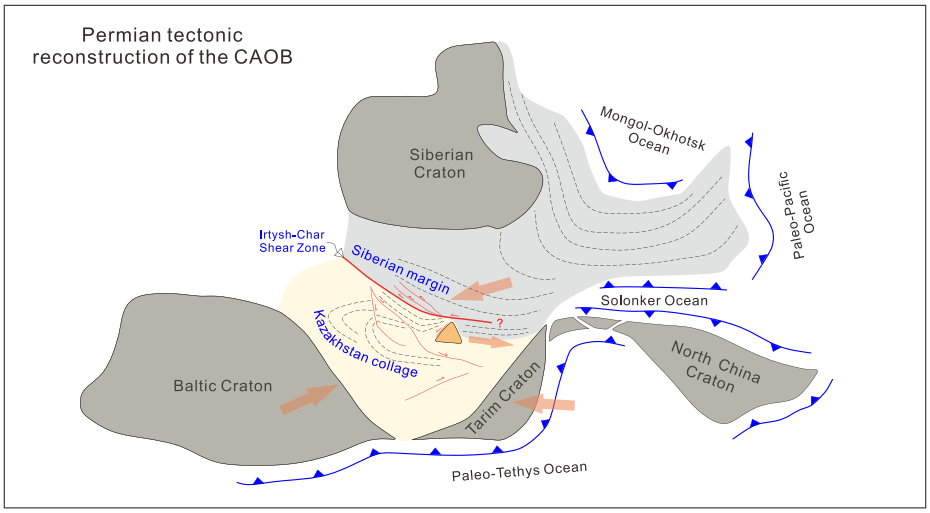

Fig. 9. Simplified tectonic reconstruction of the Central Asian Orogenic Belt in the Permian (after Xiao et al., 2015; Cunningham and Zhang, 2021). The latest Paleozoic strike-slip faulting was compatible with the eastward escape of the orogenic materials of the CAOB between the Siberian margin and the Tarim Craton (Li et al., 2015, 2017; Hu et al., 2020; He et al., 2021).

thickening and orogen-parallel extension also characterized early stage of the collision of the Siberian margin and Kazakhstan collage in eastern Kazakhstan, given the lack of detailed structural synthesis across the Irtysh-Zaisan Complex and the Zharma-Saur Arc in eastern Kazakhstan. In the scale of the whole western CAOB, the sinistral shearing along the Char, Irtysh, and North-East shear zones/faults occurred simultaneously with a series of dextral shear zones in the Tianshan Orogen farther south (Fig. 9; Shu et al., 1999; Laurent-Charvet et al., 2003; Lin et al., 2009; Wang et al., 2009; Cai et al., 2012b; Konopelko et al., 2013; Han and Zhao, 2018; Li et al., 2020, 2021; He et al., 2021). Such kinematic patterns suggest an eastward escape of orogenic segments between the Siberian margin and the Tianshan Orogen, which may link to the coeval convergence of the Siberian, Baltic, and Tarim cratons in the Permian(Li et al., 2015; Hu et al., 2020; He et al., 2021; Zhang et al., 2021).

5. Conclusions

Geochronological and Hf isotope analyses of detrital zircon samples across the Char Shear Zone provide crucial constraints for the collision of the orogenic system around the Siberian margin and the Kazakhstan collage, which are represented by the Irtysh-Zaisan Complex and the Zharma-Saur Arc/Char Zone, respectively. Carboniferous clastic rocks from the Irtysh-Zaisan Complex contain abundant early Paleozoic detrital zircons and minor Precambrian detrital zircons, which do not appear in Carboniferous sedimentary rocks of the Zharma-Saur Arc and the Char Zone. Devonian to Carboniferous detrital zircons exist in all sampling tectonic units across the Char Shear Zone, but predominant $\varepsilon_{Hf}(t)$ values of the Carboniferous detrital zircons from the Zharma-Saur Arc show a narrower range (~10–17), which is different from coeval detrital zircons within the Irtysh-Zaisan Complex (~5–18). The distinct sedimentary provenances for the Irtysh-Zaisan Complex and the Zharma-Saur Arc/Char Zone confirm that their tectonic boundary lies along the Char Shear Zone in eastern Kazakhstan. Given that the Late Carboniferous sedimentary rocks from the Zharma-Saur and the Char Zone do not contain detritus originated from the Siberian marginal orogenic system, we conclude that the Ob-Zaisan Ocean between the Siberian margin and the Kazakhstan collage was closed after the Late Carboniferous (<321 Ma) deposition in the Zharma-Saur Arc and the Char Zone.

CRediT authorship contribution statement

Wanwan Hu: Conceptualization, Methodology, Validation, Investigation, Writing – original draft, Writing – review & editing. **Pengfei Li:** Conceptualization, Methodology, Validation, Writing – review & editing, Supervision, Funding acquisition. **Min Sun:** Conceptualization, Validation, Writing – review & editing, Funding acquisition. **Inna Safonova:** Investigation, Validation, Writing – review & editing, Funding acquisition. **Yingde Jiang:** Writing – review & editing, Funding acquisition. **Chao Yuan:** Writing – review & editing, Funding acquisition. **Pavel Kotler:** Investigation, Funding acquisition.

Declaration of Competing Interest

The authors declare that they have no known competing financial interests or personal relationships that could have appeared to influence the work reported in this paper.

Acknowledgments

This study was funded by the National Natural Science Foundation of China (41872222 and 42021002), the international partnership program of the Chinese Academy of Sciences (132744KYSB20200001 and 132744KYSB20190039), Hong Kong Research Grant Council (HKU17302317), the Guangdong Province (project 2019QN01H101), and the Russian Science Foundation (project 21-77-20022 for Inna Safonova, tectonics; project 20-7710051 for Pavel Kotler, regional geology). We acknowledge Dan Wu and Le Zhang for the assistance of the analytical work. The manuscript benefits from the comments by Dongfang Song and an anonymous reviewer. This is a contribution of Guangzhou Institute of Geochemistry, Chinese Academy of Sciences (GIG-CAS; No. IS-3091), Sobolev Institute of Geology and Mineralogy SB RAS (State Assignment # 033020190003), the Chemical Geodynamics Joint Laboratory between Hong Kong University and GIG-CAS as well as IGCP 662.

Appendix A. Supplementary material

Supplementary data to this article can be found online at https://doi.org/10.1016/j.jseaes.2021.104978.

References

Abrajevitch, A., Van der Voo, R., Bazhenov, M.L., Levashova, N.M., McCausland, P.J.A., 2008. The role of the Kazakhstan orocline in the late Paleozoic amalgamation of Eurasia. Tectonophysics 455, 61–76.

Allen, M.B., Sengor, A.M.C., Natal'in, B.A., 1995. Junggar, Turfan and Alakol basins as late Permian to early Triassic extensional structures in a sinistral shear zone in the Altaid orogeic collage, central Asia. J. Geol. Soc. 152, 327–338.
Badarch, G., Dickson Cunningham, W., Windley, B.F., 2002. A new terrane subdivision for Mongolia: implications for the Phanerozoic crustal growth of Central Asia. J. Asian Earth Sci. 21, 87–110.
Bazhenov, M.L., Levashova, N.M., Degtyarev, K.E., Van der Voo, R., Abrajevitch, A.V., McCausland, P.J.A., 2012. Unraveling the early-middle Paleozoic paleogeography of Kazakhstan on the basis of Ordovician and Devonian paleomagnetic results. Gondwana Res. 22, 974–991.
Blichert-Toft, J., Albarede, F., 1997. The Lu-Hf isotope geochemistry of chondrites and the evolution of the mantle-crust system. Earth Planet. Sci. Lett. 148, 243–258.
Bold, U., Crowley, J.L., Smith, E.F., Sambuu, O., Macdonald, F.A., 2016. Neoproterozoic to early Paleozoic tectonic evolution of the Zavkhan terrane of Mongolia: Implications for continental growth in the Central Asian orogenic belt. Lithosphere 8, 729–750.
Briggs, S.M., Yin, A., Manning, C.E., Chen, Z.L., Wang, X.F., Grove, M., 2007. Late Paleozoic tectonic history of the Ertix Fault in the Chinese Altai and its implications for the development of the Central Asian Orogenic System. Geol. Soc. Am. Bull. 119, 944–960.
Buslov, M.M., Saphonova, I.Y., Watanabe, T., Obut, O.T., Fujiwara, Y., Iwata, K., Semakov, N.N., Sugai, Y., Smirnova, L.V., Kazansky, A.Y., 2001. Evolution of the Paleo-Asian Ocean (Altai-Sayan Region, Central Asia) and collision of possible Gondwana-derived terranes with the southern marginal part of the Siberian continent. Geosci. J. 5, 203–224.
Buslov, M.M., Watanabe, T., Fujiwara, Y., Iwata, K., Smirnova, L.V., Safonova, I.Y., Semakov, N.N., Kiryanova, A.P., 2004. Late Paleozoic faults of the Altai region, Central Asia: tectonic pattern and model of formation. J. Asian Earth Sci. 23, 655–671.
Buslov, M.M., Watanabe, T., Smirnova, L.V., Fujiwara, I., Iwata, K., de Grave, I., Semakov, N.N., Travin, A.V., Kir'yanova, A.P., Kokh, D.A., 2003. Role of strike-slip faults in Late Paleozoic-Early Mesozoic tectonics and geodynamics of the Altai-Sayan and East Kazakhstan folded zone. Russ. Geol. Geophys. 44, 49–75 (in Russian with the English abstract).
Cai, K.D., Sun, M., Yuan, C., Long, X.P., Xiao, W.J., 2011a. Geological framework and Paleozoic tectonic history of the Chinese Altai, NW China: a review. Russ. Geol. Geophys. 52, 1619–1633.
Cai, K.D., Sun, M., Yuan, C., Xiao, W.J., Zhao, G.C., Long, X.P., Wu, F.Y., 2012a. Carboniferous mantle-derived felsic intrusion in the Chinese Altai, NW China: Implications for geodynamic change of the accretionary orogenic belt. Gondwana Res. 22, 681–698.
Cai, K.D., Sun, M., Yuan, C., Zhao, G.C., Xiao, W.J., Long, X.P., Wu, F.Y., 2011b. Prolonged magmatism, juvenile nature and tectonic evolution of the Chinese Altai. NW China: Evidence from zircon U-Pb and Hf isotopic study of Paleozoic granitoids. 42, 949–968.
Cai, Z.H., Xu, Z.Q., He, B.Z., Wang, R.R., 2012b. Age and tectonic evolution of ductile shear zones in the eastern Tianshan-Beishan orogenic belt. Acta Petrologica Sinica 28, 1875–1895 (in Chinese with the English abstract).
Cawood, P.A., Hawkesworth, C.J., Dhuime, B., 2012. Detrital zircon record and tectonic setting. Geology 40, 875–878.
Chai, F., Mao, J., Dong, L., Yang, F., Liu, F., Geng, X., Zhang, Z., 2009. Geochronology of metarhyolites from the Kangbutiebao Formation in the Kelang basin, Altay Mountains, Xinjiang: Implications for the tectonic evolution and metallogeny. Gondwana Res. 16, 189–200.
Chen, J.F., Han, B.F., Ji, J.Q., Zhang, L., Xu, Z., He, G.Q., Wang, T., 2010. Zircon U-Pb ages and tectonic implications of Paleozoic plutons in northern West Junggar, North Xinjiang, China. Lithos 115, 137–152.
Chen, M., Sun, M., Cai, K., Buslov, M.M., Zhao, G., Rubanova, E.S., 2014. Geochemical study of the Cambrian-Ordovician meta-sedimentary rocks from the northern Altai-Mongolian terrane, northwestern Central Asian Orogenic Belt: Implications on the provenance and tectonic setting. J. Asian Earth Sci. 96, 69–83.
Chen, M., Sun, M., Cai, K., Buslov, M.M., Zhao, G., Rubanova, E.S., Voytishek, E.E., 2015. Detrital zircon record of the early Paleozoic meta-sedimentary rocks in Russian Altai: Implications on their provenance and the tectonic nature of the Altai-Mongolian terrane. Lithos 233, 209–222.
Chen, M., Sun, M., Li, P.F., Zheng, J.P., Cai, K.D., Su, Y.P., 2019. Late Paleozoic Accretionary and Collisional Processes along the Southern Peri-Siberian Orogenic System: New Constraints from Amphibolites within the Irtysh Complex of Chinese Altai. J. Geol. 127, 241–262.
Chen, Y., Xiao, W., Windley, B.F., Zhang, J.E., Sang, M., Li, R., Song, S., Zhou, K., 2017. Late Devonian-early Permian subduction-accretion of the Zharma-Saur oceanic arc, West Junggar (NW China): Insights from field geology, geochemistry and geochronology. J. Asian Earth Sci. 145, 424–445.
Choulet, F., Cluzel, D., Faure, M., Lin, W., Wang, B., Chen, Y., Wu, F.Y., Ji, W.B., 2012a. New constraints on the pre-Permian continental crust growth of Central Asia (West Junggar, China) by U-Pb and Hf isotopic data from detrital zircon. Terr Nova 24, 189–198.
Choulet, F., Faure, M., Cluzel, D., Chen, Y., Lin, W., Wang, B., 2012b. From oblique accretion to transpression in the evolution of the Altaid collage: New insights from West Junggar, northwestern China. Gondwana Res. 21, 530–547.
Choulet, F., Faure, M., Cluzel, D., Chen, Y., Lin, W., Wang, B., Xu, B., 2015. Toward a unified model of Altaids geodynamics: Insight from the Palaeozoic polycyclic evolution of West Junggar (NW China). Sci China Earth Sci 59, 25–57.
Chu, N.C., Taylor, R.N., Chavagnac, V., Nesbitt, R.W., Boella, R.M., Milton, J.A., German, C.R., Bayon, G., Burton, K., 2002. Hf isotope ratio analysis using multi-collector inductively coupled plasma mass spectrometry: an evaluation of isobaric interference corrections. J. Anal. At. Spectrom. 17, 1567–1574.
Cunningham, D., Zhang, J., 2021. China | Mongolia: Mesozoic-Cenozoic. In: David, A., Scott, A.E. (Eds), Encyclopedia of Geology, second ed., pp. 516.
Degtyarev, K.E., 2011. Tectonic evolution of Early Paleozoic island-arc systems and continental crust formation in the Caledonides of Kazakhstan and the North Tien Shan. Geotectonics 45, 23–50.
Degtyarev, K.E., Ryazantsev, A.V., 2007. Cambrian arc-continent collision in the Paleozoides of Kazakhstan. Geotectonics 41, 63–86.
Feng, Y., Coleman, R.G., Tilton, G., Xiao, X., 1989. Tectonic evolution of the West Junggar region, Xinjiang, China. Tectonics 8, 729–752.
Gebauer, D., 1996. P-T-t Path for an (Ultra-?) High-Pressure Ultramafic-Mafic Rock-Association and Its Felsic Country-Rocks Based on SHRIMP-Dating of Magmatic and Metamorphic Zircon Domains. Example: Alpe Arami(Central Swiss Alps). In: Basu, A., Hart, S. (Eds), Earth Processes Reading the Isotopic Code, pp. 307–329.
Glorie, S., De Grave, J., Delvaux, D., Buslov, M.M., Zhimulev, F.I., Vanhaecke, F., Elburg, M.A., Van den Haute, P., 2012. Tectonic history of the Irtysh shear zone (NE Kazakhstan): New constraints from zircon U/Pb dating, apatite fission track dating and palaeostress analysis. J. Asian Earth Sci. 45, 138–149.
Griffin, W.L., Pearson, N.J., Belousova, E., Jackson, S.E., van Achterbergh, E., O'Reilly, S. Y., Shee, S.R., 2000. The Hf isotope composition of cratonic mantle: LAM-MC-ICPMS analysis of zircon megacrysts in kimberlites. Geochim. Cosmochim. Acta 64, 133–147.
Han, B.F., Ji, J.Q., Song, B., Chen, L.H., Zhang, L., 2006. Late Paleozoic vertical growth of continental crust around the Junggar Basin, Xinjiang, China (part I): timing of post-collisional plutonism. Acta Petrologica Sinica 22, 1077–1086 (in Chinese with the English abstract).
Han, Y.G., Zhao, G.C., 2018. Final amalgamation of the Tianshan and Junggar orogenic collage in the southwestern Central Asian Orogenic Belt: Constraints on the closure of the Paleo-Asian Ocean. Earth-Sci. Rev. 186, 129–152.
Han, Y.G., Zhao, G.C., Sun, M., Eizenhöfer, P.R., Hou, W.Z., Zhang, X.R., Liu, D.X., Wang, B., Zhang, G.W., 2015. Paleozoic accretionary orogenesis in the Paleo-Asian Ocean: Insights from detrital zircons from Silurian to Carboniferous strata at the northwestern margin of the Tarim Craton. Tectonics 34. https://doi.org/10.1002/2014tc003668.
He, Z., Wang, B., Ni, X., De Grave, J., Scaillet, S., Chen, Y., Liu, J., Zhu, X., 2021. Structural and kinematic evolution of strike-slip shear zones around and in the Central Tianshan: insights for eastward tectonic wedging in the southwest Central Asian Orogenic Belt. J. Struct. Geol. 144 https://doi.org/10.1016/j.jsg.2021.104279.
Hu, W.W., Li, P.F., Rosenbaum, G., Liu, J.L., Jourdan, F., Jiang, Y.D., Wu, D., Zhang, J., Yuan, C., Sun, M., 2020. Structural evolution of the eastern segment of the Irtysh Shear Zone: Implications for the collision between the East Junggar Terrane and the Chinese Altai Orogen (northwestern China). J. Struct. Geol. 139 https://doi.org/10.1016/j.jsg.2020.104126.
Jahn, B.M., 2004. The Central Asian Orogenic Belt and growth of the continental crust in the Phanerozoic. Geol Soc Lond Spec Publ 226, 73–100.
Janousek, V., Jiang, Y.D., Burianek, D., Schulmann, K., Hanzl, P., Soejono, I., Kroner, A., Altanbaatar, B., Erban, V., Lexa, O., Ganchuluun, T., Kosler, J., 2018. Cambrian-Ordovician magmatism of the Ikh-Mongol Arc System exemplified by the Khantaishir Magmatic Complex (Lake Zone, south-central Mongolia). Gondwana Res. 54, 122–149.
Jiang, Y.D., Sun, M., Kröner, A., Tumurkhuu, D., Long, X.P., Zhao, G.C., Yuan, C., Xiao, W.J., 2012. The high-grade Tseel Terrane in SW Mongolia: An Early Paleozoic arc system or a Precambrian sliver? Lithos 142–143, 95–115.
Khain, E.V., Bibikova, E.V., Salnikova, E.B., Kröner, A., Gibsher, A.S., Didenko, A.N., Degtyarev, K.E., Fedotova, A.A., 2003. The Palaeo-Asian ocean in the Neoproterozoic and early Palaeozoic: new geochronologic data and palaeotectonic reconstructions. Precambr. Res. 122, 329–358.
Khromykh, S.V., Izokh, A.E., Gurova, A.V., Cherdantseva, M.V., Savinsky, I.A., Vishnevsky, A.V., 2019. Syncollisional gabbro in the Irtysh shear zone, Eastern Kazakhstan: Compositions, geochronology, and geodynamic implications. Lithos 346–347. https://doi.org/10.1016/j.lithos.2019.07.011.
Khromykh, S.V., Tsygankov, A.A., Kotler, P.D., Navozov, O.V., Kruk, N.N., Vladimirov, A. G., Travin, A.V., Yudin, D.S., Burmakina, G.N., Khubanov, V.B., Buyantuev, M.D., Antsiferova, T.N., Karavaeva, G.S., 2016. Late Paleozoic granitoid magmatism of Eastern Kazakhstan and Western Transbaikalia: plume model test. Russ. Geol. Geophys. 57, 773–789.
Konopelko, D., Seltmann, R., Apayarov, F., Belousova, E., Izokh, A., Lepekhina, E., 2013. U-Pb–Hf zircon study of two mylonitic granite complexes in the Talas-Fergana fault zone, Kyrgyzstan, and Ar–Ar age of deformations along the fault. J. Asian Earth Sci. 73, 334–346.
Kotler, P., Khromykh, S., Kruk, N., Sun, M., Li, P., Khubanov, V., Semenova, D., Vladimirov, A., 2021. Granitoids of the Kalba batholith, Eastern Kazakhstan: U-Pb zircon age, petrogenesis and tectonic implications. Lithos 388–389. https://doi.org/10.1016/j.lithos.2021.106056.
Kruk, N.N., Kuybida, M.L., Murzin, O.V., Gusev, N.I., Shokalsky, S.P., Vladimirov, A.G., Smirnov, S.Z., Gaskov, I.V., Travin, A.V., Khromykh, S.V., Volkova, N.I., Kuybida, Y. V., Annikova, I.Y., Kotler, P.D., Mikheev, E.I., 2014. Granitoids of the North-West Altai Guidebook for Field Excursion. Publishing House of Siberian Branch of the Russian Academy Sciences, p. 84.
Kruk, N.N., Rudnev, S.N., Vladimirov, A.G., Shokalsky, S.P., Kovach, V.P., Serov, P.A., Volkova, N.I., 2011. Early-Middle Paleozoic granitoids in Gorny Altai, Russia: Implications for continental crust history and magma sources. J. Asian Earth Sci. 42, 928–948.

Kuibida, M.L., Dyachkov, B.A., Vladimirov, A.G., Kruk, N.N., Khromykh, S.V., Kotler, P. D., Rudnev, S.N., Kruk, E.A., Kuibida, Y.V., Oitseva, T., 2019. Contrasting granitic magmatism of the Kalba fold belt (East Kazakhstan): Evidence for Late Paleozoic post-orogenic events. J. Asian Earth Sci. 175, 178–198.
Kuibida, M.L., Kruk, N.N., Murzin, O.V., Shokal'skii, S.P., Gusev, N.I., Kirnozova, T.I., Travin, A.V., 2013. Geologic position, age, and petrogenesis of plagiogranites in northern Rudny Altai. Russ. Geol. Geophys. 54, 1135–1148.
Kuibida, M.L., Kruk, N.N., Vladimirov, A.G., Polyanskii, N.V., Nikolaeva, I.V., 2009. U-Pb isotopic age, composition, and sources of the plagiogranites of the Kalba range, Eastern Kazakhstan. Dokl. Earth Sci. 424, 72–76.
Kuibida, M.L., Murzin, O.V., Kruk, N.N., Safonova, I.Y., Sun, M., Komiya, T., Wong, J., Aoki, S., Murzina, N.M., Nikolaeva, I., Semenova, D.V., Khlestov, M., Shelepaev, R. A., Kotler, P.D., Yakovlev, V.A., Naryzhnova, A.V., 2020. Whole-rock geochemistry and U-Pb ages of Devonian bimodal-type rhyolites from the Rudny Altai, Russia: Petrogenesis and tectonic settings. Gondwana Res. 81, 312–338.
Kuibida, M.L., Safonova, I.Y., Yermolov, P.V., Vladimirov, A.G., Kruk, N.N., Yamamoto, S., 2016. Tonalites and plagiogranites of the Char suture-shear zone in East Kazakhstan: Implications for the Kazakhstan-Siberia collision. Geosci. Front. 7, 141–150.
Laurent-Charvet, S., Charvet, J., Monié, P., Shu, L.S., 2003. Late Paleozoic strike-slip shear zones in eastern central Asia (NW China): New structural and geochronological data. Tectonics 22. https://doi.org/10.1029/2001tc901047.
Levashova, N.M., Degtyarev, K.E., Bazhenov, M.L., 2012. Oroclinal bending of the Middle and Late Paleozoic volcanic belts in Kazakhstan: Paleomagnetic evidence and geological implications. Geotectonics 46, 285–302.
Levashova, N.M., Degtyarev, K.E., Bazhenov, M.L., Collins, A.Q., Van der Voo, R., 2003. Permian palaeomagnetism of East Kazakhstan and the amalgamation of Eurasia. Geophys. J. Int. 152, 677–687.
Li, C.Y., Zhang, H., Wang, F.Y., Liu, J.Q., Sun, Y.L., Hao, X.L., Li, Y.L., Sun, W.D., 2012. The formation of the Dabaoshan porphyry molybdenum deposit induced by slab rollback. Lithos 150, 101–110.
Li, P.F., Sun, M., Rosenbaum, G., Cai, K.D., Yu, Y., 2015. Structural evolution of the Irtysh Shear Zone (northwestern China) and implications for the amalgamation of arc systems in the Central Asian Orogenic Belt. J. Struct. Geol. 80, 142–156.
Li, P.F., Sun, M., Rosenbaum, G., Cai, K.D., Yuan, C., Jourdan, F., Xia, X.P., Jiang, Y.D., Zhang, Y.Y., 2020. Tectonic evolution of the Chinese Tianshan Orogen from subduction to arc-continent collision: Insight from polyphase deformation along the Gangou section, Central Asia. Geol. Soc. Am. Bull. 132, 2529–2552.
Li, P.F., Sun, M., Rosenbaum, G., Jourdan, F., Li, S.Z., Cai, K.D., 2017. Late Paleozoic closure of the Ob-Zaisan Ocean along the Irtysh shear zone (NW China): Implications for arc amalgamation and oroclinal bending in the Central Asian orogenic belt. Geol. Soc. Am. Bull. 129, 547–569.
Li, P.F., Sun, M., Rosenbaum, G., Yuan, C., Safonova, I., Cai, K.D., Jiang, Y.D., Zhang, Y. Y., 2018. Geometry, kinematics and tectonic models of the Kazakhstan Orocline, Central Asian Orogenic Belt. J. Asian Earth Sci. 153, 42–56.
Li, P.F., Sun, M., Shu, C.T., Yuan, C., Jiang, Y.D., Zhang, L., Cai, K.D., 2019. Evolution of the Central Asian Orogenic Belt along the Siberian margin from Neoproterozoic-Early Paleozoic accretion to Devonian trench retreat and a comparison with Phanerozoic eastern Australia. Earth-Sci. Rev. 198 https://doi.org/10.1016/j.earscirev.2019.102951.
Li, P.F., Sun, M., Yuan, C., Hu, W.W., Jiang, Y.D., Jourdan, F., 2021. Late Paleozoic tectonic transition from subduction to collision in the Chinese Altai and Tianshan (Central Asia): new geochronological constrains. Am. J. Sci. 321, 178–205.
Li, S., Wang, T., Wilde, S.A., Tong, Y., 2013. Evolution, source and tectonic significance of Early Mesozoic granitoid magmatism in the Central Asian Orogenic Belt (central segment). Earth-Sci. Rev. 126, 206–234.
Li, T., Daukeev, S., Kim, B., Tomurtogoo, O., Petrov, O., 2008. Atalas of geological maps of Central Asia and adjacent areas (1:2500000).
Lin, J., Liu, Y., Yang, Y., Hu, Z., 2016. Calibration and correction of LA-ICP-MS and LA-MC-ICP-MS analyses for element contents and isotopic ratios. Solid Earth Sciences 1, 5–27.
Lin, W., Faure, M., Shi, Y., Wang, Q., Li, Z., 2009. Palaeozoic tectonics of the south-western Chinese Tianshan: new insights from a structural study of the high-pressure/low-temperature metamorphic belt. Intl J Earth Sci 98, 1259–1274.
Liu, B., Chen, J.F., Ma, X., Liu, J.L., Gong, E.P., Shi, W.G., Han, B.F., 2018. Timing of the final closure of the Irtysh-Zaysan Ocean: New insights from the earliest stitching pluton in the northern West Junggar, NW China. Geol. J. 53, 2810–2823.
Liu, Y., Hu, Z., Gao, S., Günther, D., Xu, J., Gao, C., Chen, H., 2008. In situ analysis of major and trace elements of anhydrous minerals by LA-ICP-MS without applying an internal standard. Chem. Geol. 257, 34–43.
Lobanov, K., Yakubchuk, A., Creaser, R.A., 2014. Besshi-Type VMS Deposits of the Rudny Altai (Central Asia). Econ. Geol. 109, 1403–1430.
Long, X., Yuan, C., Sun, M., Xiao, W., Wang, Y., Cai, K., Jiang, Y., 2012. Geochemistry and Nd isotopic composition of the Early Paleozoic flysch sequence in the Chinese Altai, Central Asia: Evidence for a northward-derived mafic source and insight into Nd model ages in accretionary orogen. Gondwana Res. 22, 554–566.
Long, X.P., Sun, M., Yuan, C., Xiao, W.J., Cai, K.D., 2008. Early Paleozoic sedimentary record of the Chinese Altai: Implications for its tectonic evolution. Sed. Geol. 208, 88–100.
Long, X.P., Sun, M., Yuan, C., Xiao, W.J., Lin, S.F., Wu, F.Y., Xia, X.P., Cai, K.D., 2007. Detrital zircon age and Hf isotopic studies for metasedimentary rocks from the Chinese Altai: Implications for the Early Paleozoic tectonic evolution of the Central Asian Orogenic Belt. Tectonics 26. https://doi.org/10.1029/2007tc002128.
Ludwig, K.R., 2003. Isoplot 3.00: A geochronological toolkit for Microsoft Excel.
O'Hara, K.D., Yang, X.Y., Xie, G.Y., Li, Z.C., 1997. Regional δ18O gradients and fluid-rock interaction in the Altay accretionary complex, northwest China. Geology 25, 443–446.
Qu, G.S., Zhang, J.J., 1991. Irtysh structural zone. Geosci. Xinjiang 3, 115–131 (in Chinese with the English abstract).
Qu, G.S., Zhang, J.J., 1994. Oblique thrust systems in the Altay orogen, China. J. SE Asian Earth Sci. 9, 277–287.
Rolland, Y., Alexeiev, D.V., Kröner, A., Corsini, M., Loury, C., Monié, P., 2013. Late Palaeozoic to Mesozoic kinematic history of the Talas-Ferghana strike-slip fault (Kyrgyz West Tianshan) as revealed by 40Ar/39Ar dating of syn-kinematic white mica. J. Asian Earth Sci. 67–68, 76–92.
Safonova, I., 2014. The Russian-Kazakh Altai orogen: An overview and main debatable issues. Geosci. Front. 5, 537–552.
Safonova, I., Komiya, T., Romer, R.L., Simonov, V., Seltmann, R., Rudnev, S., Yamamoto, S., Sun, M., 2018. Supra-subduction igneous formations of the Char ophiolite belt, East Kazakhstan. Gondwana Res. 59, 159–179.
Safonova, I., Kotlyarov, A., Krivonogov, S., Xiao, W.J., 2017. Intra-oceanic arcs of the Paleo-Asian Ocean. Gondwana Res. 50, 167–194.
Safonova, I., Perfilova, A., Obut, O., Kotler, P., Aoki, S., Komiya, T., Wang, B., Sun, M., 2021. Traces of intra-oceanic arcs recorded in sandstones of eastern Kazakhstan: implications from U-Pb detrital zircon ages, geochemistry, and Nd-Hf isotopes.Intl. J Earth Sci. https://doi.org/10.1007/s00531-021-02059-z.
Safonova, I., Seltmann, R., Kroener, A., Gladkochub, D., Schulmann, K., Xiao, W., Kim, J., Komiya, T., Sun, M., 2011. A new concept of continental construction in the Central Asian Orogenic Belt (compared to actualistic examples from the Western Pacific). Episodes 34, 186–196.
Safonova, I.Y., Simonov, V.A., Kurganskaya, E.V., Obut, O.T., Romer, R.L., Seltmann, R., 2012. Late Paleozoic oceanic basalts hosted by the Char suture-shear zone, East Kazakhstan: Geological position, geochemistry, petrogenesis and tectonic setting. J. Asian Earth Sci. 49, 20–39.
Saraev, S.V., Baturina, T.P., Bakharev, N.K., Izokh, N.G., Sennikov, N.V., 2012. Middle-Late Devonian island-arc volcanosedimentary complexes in northwestern Rudny Altai. Russ. Geol. Geophys. 53, 982–996.
Segal, I., Halicz, L., Platzner, I.T., 2003. Accurate isotope ratio measurements of ytterbium by multiple collection inductively coupled plasma mass spectrometry applying erbium and hafnium in an improved double external normalization procedure. J. Anal. At. Spectrom. 18, 1217–1223.
Şengör, A.M.C., Natal'in, B.A., Burtman, V.S., 1993. Evolution of the Altaid tectonic collage and Paleozoic crustal growth in Eurasia. Nature 364, 299–307.
Shen, P., Pan, H., Seitmuratova, E., Yuan, F., Jakupova, S., 2015. A Cambrian intra-oceanic subduction system in the Bozshakol area, Kazakhstan. Lithos 224–225, 61–77.
Shu, L.S., Charvet, J., Guo, L.Z., Lu, H.F., Laurent-Charvet, S., 1999. A large-scale Palaeozoic dextral ductile strike-slip zone: The Aqqikkudug-Weiya zone along the northern margin of the Central Tianshan belt, Xinjiang, NW China. Acta Geol Sin-Engl Ed 73, 148–162.
Sláma, J., Košler, J., Condon, D.J., Crowley, J.L., Gerdes, A., Hanchar, J.M., Horstwood, M.S.A., Morris, G.A., Nasdala, L., Norberg, N., Schaltegger, U., Schoene, B., Tubrett, M.N., Whitehouse, M.J., 2008. Plešovice zircon-A new natural reference material for U-Pb and Hf isotopic microanalysis. Chem. Geol. 249, 1–35.
Soejono, I., Burianek, D., Janousek, V., Svojtka, M., Cap, P., Erban, V., Ganpurev, N., 2017. A reworked Lake Zone margin: Chronological and geochemical constraints from the Ordovician arc-related basement of the Hovd Zone (western Mongolia). Lithos 294, 112–132.
Song, S., Xiao, W., Windley, B.F., Collins, A.S., Chen, Y., Zhang, J.E., Schulmann, K., Han, C., Wan, B., Ao, S., Zhang, Z., Song, D., Li, R., 2020a. Late Paleozoic Chingiz and Saur Arc Amalgamation in West Junggar (NW China): Implications for Accretionary Tectonics in the Southern Altaids. Tectonics 39. https://doi.org/10.1029/2019tc005781.
Song, S.H., Xiao, W.J., Chen, Y.C., Windley, B.F., Zhang, J.E., Chen, Z.Y., 2020b. Growth of an accretionary complex in the southern Chinese Altai: Insights from the Palaeozoic Kekesentao ophiolitic melange and surrounding turbidites. Geol. J. 56, 265–283.
Sun, M., Long, X., Cai, K., Jiang, Y., Wang, B., Yuan, C., Zhao, G., Xiao, W., Wu, F., 2009. Early Paleozoic ridge subduction in the Chinese Altai: Insight from the abrupt change in zircon Hf isotopic compositions. Sci China Ser D 52, 1345–1358.
Tong, Y., Wang, T., Siebel, W., Hong, D.W., Sun, M., 2012. Recognition of early Carboniferous alkaline granite in the southern Altai orogen: post-orogenic processes constrained by U-Pb zircon ages, Nd isotopes, and geochemical data. Int. J. Earth Sci. 101, 937–950.
Travin, A.V., Boven, A., Plotnikov, A.V., Vladimirov, V.G., Theunissen, K., Vladimirov, A. G., Melnikov, A.I., Titov, A.V., 2001. $^{40}Ar/^{39}Ar$ dating of ductile deformations in the Irtysh shear zone, eastern kazakhstan. Geochem. Int. 12, 1237–1241 (in Russian).
Vladimirov, A.G., Kruk, N.N., Khromykh, S.V., Polyansky, O.P., Chervov, V.V., Vladimirov, V.G., Travin, A.V., Babin, G.A., Kuibida, M.L., Khomyakov, V.D., 2008. Permian magmatism and lithospheric deformation in the Altai caused by crustal and mantle thermal processes. Russ. Geol. Geophys. 49, 468–479.
Volkova, N.I., Tarasova, E.N., Polyansky, N.V., Vladimirov, A.G., Khomyakov, V.D., 2008. High-pressure rocks in the serpentinite melange of the Chara zone, Eastern Kazakhstan: Geochemistry, petrology, and age. Geochem. Int. 46 (4), 386–401.
Wan, B., Zhang, L., Xiang, P., 2010. The Ashele VMS-type Cu-Zn Deposit in Xinjiang, NW China Formed in a Rifted Arc Setting. Resour. Geol. 60, 150–164.
Wang, B., Cluzel, D., Shu, L., Faure, M., Charvet, J., Chen, Y., Meffre, S., De Jong, K., 2009. Evolution of calc-alkaline to alkaline magmatism through Carboniferous convergence to Permian transcurrent tectonics, western Chinese Tianshan. Intl J Earth Sci 98, 1275–1298.

Wang, T., Hong, D.W., Jahn, B.M., Tong, Y., Wang, Y.B., Han, B.F., Wang, X.X., 2006. Timing, petrogenesis, and setting of Paleozoic synorogenic intrusions from the Altai Mountains, northwest China: Implications for the Tectonic evolution of an accretionary orogen. J. Geol. 114, 735–751.

Wang, T., Tong, Y., Li, S., Zhang, J.J., Shi, X.X., Li, J.Y., Han, B.F., Hong, D.W., 2010. Spatial and temporal variations of granitoids in the Altay orogen and their implications for tectonic setting and crustal growth:perspectives from Chinese Altay. 29, 595–618 (in Chinese with the English abstract).

Wang, Y., Yuan, C., Long, X., Sun, M., Xiao, W., Zhao, G., Cai, K., Jiang, Y., 2011. Geochemistry, zircon U-Pb ages and Hf isotopes of the Paleozoic volcanic rocks in the northwestern Chinese Altai: Petrogenesis and tectonic implications. J. Asian Earth Sci. 42, 969–985.

Wang, Y.W., Wang, J.B., Wang, L.J., Long, L.L., Tang, P.Z., Liao, Z., Zhang, H.Q., Shi, Y., 2012. The Tuerkubantao ophiolite mélange in Xinjiang, NW China: New evidence for the Erqis suture zone. Geosci. Front. 3, 587–602.

Wei, W., Pang, X., Wang, Y., Xu, B., 2009. Sediment facies, provenance evolution and their implications of the Lower Devonian to Lower Carboniferous in Shaerbuerti mountain in North Xinjiang. Acta Petrologica Sinica 25, 689–698 (in Chinese with the English abstract).

Wilhem, C., Windley, B.F., Stampfli, G.M., 2012. The Altaids of Central Asia: A tectonic and evolutionary innovative review. Earth-Sci. Rev. 113, 303–341.

Windley, B.F., Alexeiev, D., Xiao, W.J., Kröner, A., Badarch, G., 2007. Tectonic models for accretion of the Central Asian Orogenic Belt. J. Geol. Soc. London 164, 31–47.

Windley, B.F., Kroner, A., Guo, J.H., Qu, G.S., Li, Y.Y., Zhang, C., 2002. Neoproterozoic to Paleozoic geology of the Altai orogen, NW China: New zircon age data and tectonic evolution. J. Geol. 110, 719–737.

Wu, F.Y., Yang, Y.H., Xie, L.W., Yang, J.H., Xu, P., 2006. Hf isotopic compositions of the standard zircons and baddeleyites used in U-Pb geochronology. Chem. Geol. 234, 105–126.

Wu, Y.B., Zheng, Y.F., 2004. Genesis of zircon and its constraints on interpretation of U-Pb age. Chin. Sci. Bull. 49, 1554–1569 (in Chinese with the English abstract).

Xiao, W., Han, C., Yuan, C., Sun, M., Zhao, G., Shan, Y., 2013. Transitions among Mariana-, Japan-, Cordillera- and Alaska-type arc systems and their final juxtapositions leading to accretionary and collisional orogenesis. In: Kusky, T. M., Zhai, M. G., Xiao, W. (Eds). Evolving Continents: Understanding Processes of Continental Growth. Geological Society Special Publication 338, pp. 35–53.

Xiao, W.J., Huang, B.C., Han, C.M., Sun, S., Li, J.L., 2010. A review of the western part of the Altaids: A key to understanding the architecture of accretionary orogens. Gondwana Res. 18, 253–273.

Xiao, W.J., Windley, B.F., Han, C.M., Liu, W., Wan, B., Zhang, J.E., Ao, S.J., Zhang, Z.Y., Song, D.F., 2018. Late Paleozoic to early Triassic multiple roll-back and oroclinal bending of the Mongolia collage in Central Asia. Earth-Sci. Rev. 186, 94–128.

Xiao, W.J., Windley, B.F., Sun, S., Li, J.L., Huang, B.C., Han, C.M., Yuan, C., Sun, M., Chen, H.L., 2015. A Tale of Amalgamation of Three Permo-Triassic Collage Systems in Central Asia: Oroclines, Sutures, and Terminal Accretion. Annu. Rev. Earth Planet. Sci. 43, 477–507.

Yang, G., Li, Y., Safonova, I., Yi, S., Tong, L., Seltmann, R., 2014. Early Carboniferous volcanic rocks of West Junggar in the western Central Asian Orogenic Belt: implications for a supra-subduction system. Int. Geol. Rev. 56, 823–844.

Yang, T.N., Li, J.Y., Zhang, J., Hou, K.J., 2011. The Altai-Mongolia terrane in the Central Asian Orogenic Belt (CAOB): A peri-Gondwana one? Evidence from zircon U-Pb, Hf isotopes and REE abundance. Precambr. Res. 187, 79–98.

Yu, Y., Sun, M., Huang, X.L., Zhao, G.C., Li, P.F., Long, X.P., Cai, K.D., Xia, X.P., 2017. Sr-Nd-Hf-Pb isotopic evidence for modification of the Devonian lithospheric mantle beneath the Chinese Altai. Lithos 284–285, 207–221.

Yuan, C., Sun, M., Xiao, W.J., Li, X.H., Chen, H.L., Lin, S.F., Xia, X.P., Long, X.P., 2007. Accretionary orogenesis of the Chinese Altai: Insights from Paleozoic granitoids. Chem. Geol. 242, 22–39.

Zhang, C.L., Santosh, M., Zou, H.B., Xu, Y.G., Zhou, G., Dong, Y.G., Ding, R.F., Wang, H. Y., 2012. Revisiting the "Irtish tectonic belt": Implications for the Paleozoic tectonic evolution of the Altai orogen. J. Asian Earth Sci. 52, 117–133.

Zhang, B.H., Zhang, J., Zhao, H., Qu, J.F., Zhang, Y.P., Niu, P.F., Hui, J., Yun, L., 2021. Kinematics and geochronology of Late Paleozoic-Early Mesozoic ductile deformation in the Alxa Block, NW China: new constraints on the evolution of the Central Asian Orogenic Belt. Lithosphere. https://doi.org/10.2113/2021/3365581.

Zhang, D., Zhou, T., Yuan, F., Deng, Y., Xu, C., Zhang, R., Li, P., Wang, J., 2015a. The discovery on the Early Paleozoic magmatism in the Sawuer area, West Jungaar. Acta Petrologica Sinica 31, 415–425 (in Chinese with the English abstract).

Zhang, L., Ren, Z.-Y., Nichols, A.R.L., Zhang, Y.-H., Zhang, Y., Qian, S.-P., Liu, J.-Q., 2014. Lead isotope analysis of melt inclusions by LA-MC-ICP-MS. J. Anal. At. Spectrom. 29, 1393–1405.

Zhang, L., Ren, Z.-Y., Xia, X.-P., Li, J., Zhang, Z.-F., 2015b. IsotopeMaker: A Matlab program for isotopic data reduction. Int. J. Mass Spectrom. 392, 118–124.

Zhang, Y., Li, P., Sun, M., Yuan, C., 2020. Late Paleozoic to early Triassic granitoids from the Rudny Altai, Central Asian Orogenic Belt: Petrogenesis and implications for continental crustal evolution. Solid Earth Sciences 5, 115–129.

Zhou, T., Yuan, F., Fan, Y., Zhang, D., Cooke, D., Zhao, G., 2008. Granites in the Sawuer region of the west Junggar, Xinjiang Province, China: Geochronological and geochemical characteristics and their geodynamic significance. Lithos 106, 191–206.

Zhou, T., Yuan, F., Zhang, D., Deng, Y., Xu, C., Zhang, R., Guo, X., Li, P., 2015. Genesis of the granitoids intrusions in Tabei area, West Junggar, Northwest China: Evidences from geological and geochemical characteristics. Acta Petrologica Sinica 31, 351–370 (in Chinese with the English abstract).

Zhu, Y., Xu, X., 2006. The discovery of Early Ordovician ophiolite melange in Taerbahatai Mts., Xinjiang, NW China. Acta Petrol. Sin. 22, 2833–2842 (in Chinese with the English abstract).

Zonenshain, L.P., Kuzmin, M.I., Natapov, L.M., Page, B.M., 1990. Geology of the USSR: A Plate-Tectonic Synthesis. Am. Geophys. Union Geophys. Monogr. 21 https://doi.org/10.1029/GD021.